Indentation Behavior of Tubular Members

by

Joseph A. Padula
Alexis Ostapenko

Sponsored by

Minerals Management Service
of the U.S. Department of the Interior
(Contract No. 14-12-0001-30288)
and
American Iron and Steel Institute
(Project No. 338)

DOI/AISI COOPERATIVE RESEARCH PROGRAM

Fritz Engineering Laboratory Report No. 508.8

Lehigh University

June 1988

Table of Contents

List of Figures

List of Tables

Abstract

The "damage design" approach to offshore structure design requires consideration of accidental damage and its effect on the structural integrity. For this reason, an experimental and analytical investigation of the indentation behavior of tubular members was conducted.

The experimental work consisted of the indentation of two large-diameter steel specimens which were fabricated by cold-rolling and welding. The test specimens were 1.0 m (40 in.) and 1.5 m (60 in.) in diameter with the corresponding D/t ratios of 151 and 227. Each specimen was simply supported at its ends and subjected to a lateral load applied through a rigid indenter at midlength. Load-deformation response and the energy absorption as functions of dent depth were obtained.

The analytical work included the finite element analysis of the indentation of the two test specimens and of three additional specimens whose indentation response was reported in literature. In contrast to the two fabricated test specimens, these three specimens were manufactured and stress relieved.

The agreement between the analytical and experimental load vs. dent depth responses was much better for the manufactured tubes compared to the fabricated specimens. This observation prompted an investigation into the effect of residual stresses (due to cold-rolling during fabrication) on the indentation response. It was shown that these residual stresses can significantly affect the load-deformation relationship by reducing the amount of energy absorbed for a given dent depth. Consequently, neglecting their effect can result in an underestimation of the damage resulting from a given "design collision".

A simplified analytical method for estimating the load vs. dent depth response of tubular members subjected to "knife-edge" loading was developed. Prediction of the load-deformation behavior is given by a three-term polynomial whose coefficients are readily determined from the geometric and material characteristics of the member. The method is based on a regression analysis of experimental data taken from available literature.

1. Introduction

In the design of offshore platforms, it is necessary to consider the possibility of structural damage resulting from accidental impact during construction or operation, a ship/platform collision, ice hazards, or severe cases of overloading. Of these, ship/platform collisions occur fairly frequently and are probably the single most common type of offshore accident resulting in structural damage. [5] Although it may be impractical to design structures to resist a collision with a large vessel such as a tanker and sustain only moderate damage, the design process must include consideration of the more probable collisions with supply vessels or other light ship traffic. The objective would be to limit the extent of damage so that the integrity of the structure is not significantly compromised or that it can be maintained until repairs can be effected. This requires that the designer be able to estimate the extent of damage that may be expected as well as the residual strength of the structure after damage.

Requiring that the structural integrity of a platform be maintained in the event of an accidental collision necessitates that the structure have sufficient capacity to sustain elastic and plastic deformations thereby providing a mechanism for absorption of energy. Even though elastic deformations and/or vibrations may dissipate most of the energy from minor ship/platform collisions or accidental impacts, plastic deformations will develop at least at the point of contact. [5]

1.1 Scope

To determine the effect of damage, it is first necessary to have some, at least approximate, knowledge of the type and extent of damage that can be reasonably expected as a result of a collision. In structures framed with steel tubular members, the result of a collision usually takes the form of localized dents and/or overall deflection of a member(s). The interaction of these two deformation modes is complex and

depends on the geometry of the member, the end restraint interaction by the frame, and the type of the event producing damage.

With the knowledge of the member/structure response, in an impact or collision, the energy absorption capacity can be determined and thereby provide a means for estimating the extent of damage given a "design collision" with a known mass and velocity. Therefore, determination of the load deformation response and energy absorption capacity of a structure is a prerequisite to prudent design. For these reasons, the current research has been focused on the determination of the indentation behavior of tubular steel members.

1.2 Previous Work

A number of researchers have investigated the indentation of tubular members as it relates to accidental damage in offshore structures. [14, 13, 12, 16, 17] Lateral loading of tubular members and the resulting deformation mechanisms have been the focus of much of this research. The approaches to the problem range from the development of simplified analytical models and the use of numerical techniques such as the finite element method to experimental work. For example, Taby's work on the residual strength of damaged tubular members has involved extensive experimental work including the indentation of tubular members. [15] On the other hand, Wierzbicki and Suh have presented a purely theoretical analysis of the denting of tubular members under combined bending and axial loading. [17] Soares and Soreide have presented a simplified analysis of tubular members whose primary mode of deformation was overall beam deflection and a correlation of the results with finite element analysis. [13] An excellent review of the state of the art of the collision-damage and residual strength of offshore structures including a comprehensive bibliography has been provided by Ellinas. [5]

Since they are usually based on simplifying idealizations, the proposed analytical models must be validated by correlation with experimental results before they can be used with confidence. The idealizations used may range from the common assumption of rigid-plastic material behavior to a prescribed deformation geometry. Due to the complex interaction of localized denting and overall bending deformation, and the wide range of tube geometries and loadings, such assumptions may affect the accuracy of the analytical model.

The need for the correlation of theoretical with experimental results also applies to the results obtained from numerical techniques such as the finite element method. Additionally, the use of the finite element method for generating solutions for such a complex problem involving material and geometric nonlinearities requires considerable expense in terms of time and computer resources.

Probably the most significant shortcoming of the experimental research reported so far is the lack of work on tubular members fabricated by cold-rolling and welding, which is the usual method of fabrication for offshore structures, and of the consideration of members with large D/t ratios. The work described here addresses these needs, at least in part.

1.3 Present Investigation

The thrust of the current research effort has been to determine the response of tubular members under a lateral load assuming the primary mode of deformation to be localized denting of the tube wall. This investigation consisted of experimental and analytical phases. The results of the analytical work were correlated with the experimental work of the current project as well as with the experimental results reported by Taby and Rashed in Reference [14]. A brief description of the experimental work performed by Taby and Rashed is given in Appendix A. The experimental data

reported in Reference [14] was also used to develop a simplified approximate method for predicting the load vs. dent depth response.

1.3.1 Experimental Work

The experimental phase of the project involved the testing of two large-diameter, fabricated tubular test specimens. Each specimen was subjected to a lateral load at mid-length to produce a localized indentation. The specimens were simply supported at the ends and the load was applied through a rigid indenter. The displacements were measured at several locations thus providing the necessary data to establish the load vs. dent-depth and the energy dissipation relationships. The indentation of the test specimens was also a prelude to further experimentation (axial load testing) on the residual strength of damaged tubular members. [10]

1.3.2 Analytical Work

The analytical work consisted of the finite element analysis of the indentation of tubular members and the correlation of the results with experimental data. In order to assess the validity of the finite element analysis over a wide range of tube geometries and material properties, the analysis and correlation were made for five specimens for which experimental data were available; two specimens tested as a part of this program and three specimens for which load vs. dent depth curves were taken from Reference [14]. Correlation with experimental data also provided useful information for the refinement of the modeling technique.

The effect of residual stresses caused by cold-rolling during the fabrication process on the load vs. dent depth response was also investigated. This was prompted by a much better correlation between the results of the finite element analysis and the experimental data from the manufactured and stress relieved test specimens reported in Reference [14] as compared to the correlation with the data from the fabricated

specimens of the experimental phase of the current work. The investigation demonstrated that residual stresses can have a significant effect on the indentation response. Specifically, the residual stresses reduce the stiffness of the response, and, thus, neglecting their effect can result in an underestimation of the damage caused by a given "design collision".

A simplified approximate method for predicting the denting response of tubular members subjected to a lateral load with a "knife-edge" indenter was developed. The load-deformation response is predicted by a three term approximating function whose coefficients are readily calculated from the geometric and material properties of the member. The matrix for calculating the coefficients of the approximating function and the approximating function itself were determined by a regression analysis of the experimental data reported in Reference [14].

2. Experimental Work

The experimental work consisted of the indentation of two large-diameter, fabricated specimens. The load vs. dent depth response of the specimens was recorded and the energy absorption as a function of dent depth was calculated.

Additional experimental data consisting of the indentation response of three specimens (Specimens IIICI, IBII, and IIAII) were taken from Reference [14] for correlation with the analytical work. A brief description of this experimental work is given in Appendix A.

2.1 Description of Test Specimens

The specimens were obtained by modifying two test specimens of a previous project (Specimens T3 and T4 in References [8, 6]). For the current project, these two specimens were designated P1 and P2, respectively.

2.1.1 Fabrication and Modification of Test Specimens

The two test specimens, P1 and P2, were fabricated by cold-rolling steel plate into right circular cylinders in a pyramid three-roller bending machine and welding the longitudinal seam by an automatic submerged-arc process. Steel end rings were welded to the ends of the specimens to facilitate uniform distribution of the axial load during testing. Detailed information on the fabrication and material properties is given in Reference [8].

Previous axial load testing resulted in severe local buckles confined to one end of each specimen. The limited extent of the deformations made it possible to modify these specimens for reuse by removing the buckled portions and reattaching the end rings. The modification process is further described in Reference [10].

2.1.2 Dimensions and Material Properties

Specimens P1 and P2 had outside diameters of 1.02 m (40.2 in.) and 1.53 m (60 in.), respectively. Both specimens had a wall thickness of 6.73 mm (0.265 in.). After modification, Specimen P1 was 2.44 m (96 in.) long and Specimen P2 2.13 m (84 in.), exclusive of the thickness of the end rings. The circular steel end rings welded to the ends of the specimens were 22 mm thick by 127 mm wide (7/8 in. x 5 in.). All pertinent geometric and material properties including diameter-to-thickness (D/t), length-to-radius of gyration (L/r) and dent depth-to-diameter (d/D) ratios are listed in Table 1.

The specimens were fabricated from ASTM A36 steel plate. In previous research the static and dynamic yield stresses of the material were determined from standard ASTM coupons. [8] The material properties of the modified specimens were assumed to be the same as those of the original specimens. Thus, the possible effect of work hardening during the original tests was neglected.

2.2 Indentation of Test Specimens

The indentation of the specimens was accomplished by the application of a lateral load through a rigid indenter. The load vs. dent depth relationship and the energy absorption as a function of the dent depth were determined from the test data.

2.2.1 General Considerations

Although damage to a tubular member due to impact may result in localized dents, overall deflection or a combination of both, the experimental phase of this project dealt only with localized denting. Consequently, the indentation of the specimens was undertaken with the goal of producing dents with as little overall distortion of the member as possible.

Consideration was given to various dent geometries, e.g., vee (resulting from a "knife edge" loading), rounded or flat. The selected shape was a localized flattening as shown in Fig. 3. The flat portion of the dent, measured longitudinally along the specimen, was 175 mm (7 in.) in width. The length of the dent (measured transversely across the specimen) was largely controlled by the depth and was approximately equal to the chord distance subtended by a circular arc with a middle ordinate equal to the dent depth.

The dent was located at mid-length of each specimen. The longitudinal centerline of the dent was offset by 120° of arc from the longitudinal weld seam. (The actual location for Specimen P1 was approximately 38 mm (1.5 in.) closer to the weld seam.)

2.2.2 Arrangement and Procedure for Indentation of Specimens

The arrangement for indentation was designed to introduce a dent and to obtain data on the deformation and energy dissipation characteristics of the test specimens. The same set-up was used for both specimens; it consisted of a reaction frame, a load transmission assembly and instrumentation.

The set-up was made in a universal testing machine which served as the reaction frame. As shown in Fig. 1, the test specimen was placed horizontally on the floor of the testing machine and supported by steel blocks under the end rings. The blocks, in effect, provided simple support at the ends of the specimen and also gave the necessary clearance to place dial gages underneath the specimen.

The load transmission assembly between the testing machine head and the specimen consisted of a short section of wide flange beam placed transversely across the specimen, a manually operated hydraulic jack, and a load cell. The 175 mm (7 in.)

wide flange of the beam served as the die for forming the dent. A view of the indentation of Specimen P2 in progress is shown in Fig. 2. The test setup is shown schematically in Fig. 4. Internal bracing with struts and transverse bearing members was installed at the edges of the intended indentation in order to localize the deformation.

The instrumentation for measuring the deformation of the specimens during indentation consisted of ten mechanical dial gages located as shown in Fig. 4. Two were placed between the beam and the testing machine head, one on each side of the jack-loadcell assembly. These gages directly measured the extension of the jack and, thus, the displacement relative to the machine head. Four dial gages were placed between the top surface of the specimen and the testing machine head, and three between the testing machine floor and the bottom of the specimen. One dial gage was used to directly measure the displacement of the machine head relative to the floor. This was done by connecting a dial gage mounted on a pedestal on the floor with a light-gage wire to a magnetic clip on the testing machine head.

The indentation procedure consisted of incremental application of load to the specimen through the jack-loadcell-beam assembly. At each load increment, the load and dial gage readings were recorded. The approximate depth of dent was indicated by the readings from the dial gages between the machine head and the beam. Loading continued until the dent exceeded the desired depth by an amount estimated to be lost due to the elastic recovery during unloading. The set-up and procedure for indentation were similar for both specimens.

Specimen P1 required two cycles of loading and unloading because the elastic recovery was underestimated in the first cycle. The observed elastic recovery during the first unloading provided a means of more accurately estimating the final dent

depth. The maximum load needed for P1 to develop the desired dent depth was 168 kN (37.8 kips).

During loading of Specimen P2, at approximately 160 kN (36 kips), one of the wooden struts used for internal bracing failed unexpectedly, and the load immediately dropped to 116 kN (26 kips). The specimen was then unloaded, the wooden struts replaced with steel members, and loading continued to 276 kN (62 kips).

Plots of the load vs. dent depth for the specimens are shown in Figs. 5 and 6. The load was non-dimensionialized with respect to a factor $\left(\frac{4D^2t\sigma_y}{L}\right)$, the magnitude of a concentrated load at midspan which would produce a plastic moment according to simple beam theory. The dent depth is given as a fraction of the tube diameter.

2.2.3 Results of Indentation

The indentation tests produced localized dents at midlength of the two specimens as well as data on the load vs. dent depth response. The energy dissipation as a function of dent depth was also determined.

2.2.3.1 Dent Geometry

Locally, the final depth of dent for Specimen P1 was 19 mm (0.75 in.), the depth being measured with respect to the points just outside the dented area. Subsequent measurements of the specimen geometry with respect to the ends of the specimen showed that the overall depth of indentation was 28 mm (1.1 in.). This indicated that the deformation was a combination of a local dent and an overall deflection of the specimen wall. For Specimen P2, the depth of dent was 70 mm (2.8 in.) locally and 84 mm (3.3 in.) overall.

Thus, the nature of the dent was also predominantly local with only a slight overall distortion of the specimen. The dentdepth-to-diameter ratios for Specimens P1 and P2 were 2.7% and 5.5%, respectively.

The surfaces of the dented specimens were mapped with contour plots. A complete description of the dent geometry of both specimens, including the surface contour plots, is given in Reference [10].

2.2.3.2 Energy Dissipation

The amount of energy dissipated during the indentation process was determined from the area under the load vs. dent depth curve. Figure 7 shows the total energy absorbed vs. the dent depth for each specimen. The total energy absorbed included both the elastic and plastic deformations since this would be of interest in considering the mechanics of a collision.

3. Finite Element Analysis

In order to investigate the tube indentation problem analytically, finite element models were developed and solutions obtained using the 1981 version of the program ADINA.* This program was selected because of its capability to consider material and geometric nonlinearities. The analysis was performed on a Control Data Corporation Cyber 180 Model 850 computer running the NOS and NOS/VE operating systems.

The indentations of Specimens P1 and P2 as well as of Specimens IBII, IIAII, IIICI were analyzed. Pertinent information on the latter three specimens, which are a representative sampling of the specimens tested by Taby and Rashed, is given in Appendix A and Reference [14]. These five specimens covered a wide range of tube geometries and material properties and provided the experimental data for comparison with the results of the analysis.

3.1 Introduction

The response of a tubular member subjected to indentation is highly nonlinear due to the large deformations of the tube and plastification of the material. The analysis is also complicated by the nature of the contact between the indenter and the tube wall. The contact area increases with the dent depth and the distribution of the load over the contact surface is continuously changing. Because the contact area and the distribution of the load are both dependent on the response of the tube, the applied load (actually, an induced nodal point displacement) could not be given as prescribed input for the computer program. Consequently, a modeling technique similar to that employed by Hypponen and Raiko in the analysis of a pipe whipping against a rigid support was used. [7] The material and geometric nonlinearities due to plastifica-

*ADINA Engineering AB, Vasteras, Sweden, and ADINA Engineering Inc., Watertown, Massachusetts

tion and large deformations were within the capabilities of ADINA, and the difficulty was only in determining the computational parameters such as load increments and convergence tolerances.

3.2 Modeling

The finite element model consisted of two basic components: an assemblage of shell elements representing the tube and a set of truss elements designed to model the contact between a rigid indenter and the tube wall. Isoparametric shell elements with variable number of nodes from the ADINA element library were used to model the tube. The rigid indenter was modeled with two-node truss elements having nonlinear material properties. The internal braces used during the indentation of Specimens P1 and P2 were modeled with single linearly elastic truss elements.

Due to the double symmetry of the problem, only one fourth of the tube needed to be modeled. The tube was sectioned along the longitudinal and transverse planes of symmetry which passed through the center of the indentation. An overall view of a typical model is shown in Fig. 8.

3.2.1 Contact Problem

The problem of modeling the contact of a rigid indenter against a cylindrical tube was simulated by a series of truss elements with nonlinear material properties. At one end, the truss elements were connected to the shell element nodal points in the indentation area of the tube wall. The opposite ends of all the truss elements were connected to a common node at a sufficient distance from the surface of the tube to consider the line of action of the forces to be parallel. A prescribed displacement was imposed on this node to produce the indentation of the tube. (See Fig. 8)

The truss elements used to model the indentation of Specimens P1 and P2 were

arranged in three rows corresponding to the 175 mm (7 in.) width of the indenter. Since the specimens tested by Taby were subjected to a knife edge loading, the indentation was modeled with a single row of truss elements on the centerline of the indentation.

Simulation of the contact was achieved through the definition of the constitutive relationship for the truss elements. Nonlinear elastic material property defined by a piecewise-linear stress-strain (σ-ϵ) relationship was selected from the material models available for truss elements in ADINA. Pairs of σ-ϵ values input into the program defined the stress and tangent modulus as functions of strain.

A typical stress-strain diagram for a truss element is shown in Fig. 9. To model the condition of contact (no tension forces may develop between the tube surface and the indenter), the truss elements were made extremely soft in tension by defining a very small modulus of elasticity for positive strains. Modeling of the initial gap between the indenter and the tube was accomplished by extending the soft material response into the compression range. After the contact between the indenter and tube wall was established, the modulus of elasticity was made very large. Typically, as shown in Fig. 9, this range was preceded by a short transition of moderate stiffness.

The values of ϵ_s, the strain at which the modulus of elasticity increases to its maximum value, were determined for each truss element from the geometry as shown in Fig. 10, where $\epsilon_s = \frac{\delta}{L}$. The transition from an essentially zero modulus of elasticity to rigid was also determined from the geometry. The value of ϵ_s calculated for a truss element marked the initiation of the transitional stiffness for the adjacent truss element. This constitutive relationship allowed the truss elements to have virtually no stiffness until the deformed geometry of the model was consistent with contact at a nodal point by a rigid indenter.

The use of a transition in the stress-strain relationships proved to be computationally expedient and was also justified in the simulation of the physical problem. In a direct comparison of analyses with trilinear and bilinear stress-strain curves, that is, with and without a transition, the bilinear relationship was slightly more costly, requiring 4% more CPU time for a 13% increase in the number of equilibrium iterations. Also, the calculated load vs. dent depth response with the trilinear stress-strain relationship was considerably smoother.

The physical justification for using the transition in moduli of elasticity lies in the continuous nature of the actual distributed loading as opposed to the application of the load at discrete nodal points. The transition simulates a continuous loading by allowing a more gradual shifting of the load from one nodal point to the next as the dent depth is increased. For this reason, a quad-linear stress-strain relationship (2 transitions) was used in the analyses performed with Model 2 which had a somewhat coarser mesh in the area of indentation (See Sec. 3.4.3).

3.2.2 Discretization of the Tube

Excluding some preliminary models, three discretizations of the tube were used. One model was used only for the analysis of test specimens P1 and P2, while two other, more refined models, were used in the analysis of all five specimens. The latter two models differed from the first by the type of shell elements and by the coarseness of the mesh at the indentation. The principal difference between the two latter discretizations was basically a modification to accommodate larger dent depths.

A description of the three models is given in the following paragraphs. In the course of the work, these models were somewhat arbitrarily given the designations Model 2, 4, and 8 corresponding to a scheme for labeling each of the computer runs made. Dimensions related to the discretization for each model and to the particular specimens are shown in unfolded views of the meshes in Figs. 11, 12 and 13.

Model 2, the model first used for the analysis of Specimens P1 and P2, consisted of 32 shell elements and 150 nodal points as shown in Fig. 14. Nine-node shell elements were employed, except for the two elements used as a transition to a finer mesh at the indentation. At the indentation, the circumferential discretization consisted of two elements spanning 20° of arc. Thus, three rows of five nodal points in the circumferential direction were connected to the truss elements. The remaining 160° of arc consisted of two elements of 20° and three elements of 40°.

The discretization of Model 4 shown in Fig. 15 consisted of 26 shell elements which, except for the transition elements, were 16-node elements. Thus, this model had a total of 196 nodal points. Due to the much finer mesh in the region of indentation the response produced by this model was much smoother than by Model 2. The circumferential discretization at the indentation consisted of six elements spanning 5° of arc each followed by one element with 30° and two elements with 60°. The effect of the finer mesh was an improved simulation of the continuous application of a load distributed over the surface of the tube because of the denser population of truss elements transmitting load to the shell as well as an increased sensitivity to deformations. The use of 16-node shell elements also permitted a more rapid transition from the fine mesh over the indentation to a coarser mesh away from the dented area.

The third discretization, Model 8, was used to accommodate larger relative dent depths. This model, shown in Fig. 16, is a modification of Model 4 with the fine mesh in the region of indentation extending over 60° of arc as opposed to 30°. The mesh in this region was slightly coarser since only six elements in the circumferential direction were used over 60° of arc. This model consisted of 28 shell elements, typically, 16-node, and a total of 227 nodal points.

3.3 Boundary Conditions

The boundary conditions imposed on the models were dictated by two criteria; the enforcement of deformations consistent with the symmetry of the problem and the imposition of the support conditions of the two different test arrangements used for the indentation of Specimens P1 and P2 (See Sec. 2.2) vs. Specimens IIICI, IBII, and IIAII (See Appendix A).

The boundary conditions required to impose the condition of symmetry on the quarter section model were the same for all five specimens. At the circumferential cut made by the transverse plane of symmetry at the center of indentation, the translational degree of freedom in the longitudinal direction and rotation about a tangent to the circumference were prevented. Along the two longitudinal cuts made by the longitudinal plane of symmetry, the translation in the circumferential direction, as well as, the rotation about the longitudinal axis were prevented.

The support conditions of the test setup for Specimens P1 and P2 were modeled by preventing translation in the transverse plane at the end of the model. This accommodated the effect of the support arrangement as well as of the end rings attached to these two specimens (See Chap. 2).

The support arrangements for the indentation and the length of the Specimens IIICI, IBII, and IIAII (See Appendix A), permitted the analytical models to be shortened for the sake of economy of computation. The length of the models was made not less than one and a half diameters since the portions of the tube outside this region would have negligible effect on the indentation. The actual lengths of the models used for these three specimens are given in Figs. 12 and 13. All degrees of freedom were allowed at the truncated free end of the model. The cradle support for these specimens was modeled by prohibiting translation in the radial direction at the nodal points directly opposite the indentation.

3.4 Computational Parameters

The high degree of nonlinearity of the problem resulting from large displacements coupled with material nonlinearity and the aforementioned contact problem presented some computational difficulties. When unresolved, these difficulties typically manifested themselves in an erratic calculated response or an abnormal termination of computation. However, useful results were obtained after gaining some experience with the application of the computer program to these models. In particular, some experimentation was necessary to determine the effect of the various user input parameters which relate to the formulation and solution of the incremental equilibrium equations. In general, the load increments had to be made very small and equilibrium iterations performed at every load step. The stiffness matrix was also updated at every load step. Even with these measures taken, the calculated response was not always as smooth as would be desired.

3.4.1 Formulation of Equations

For the shell elements, total Lagrangian formulation was used (large displacements and rotations with small strains) together with elasto-plastic material behavior. The von Mises yield criterion was used for the material model. [2]

In the formulation of the element matrices, ADINA employs Gauss numerical integration for which the order of integration (number of integration points) is controlled by the analyst. The program documentation offers somewhat nebulous advice on suggested integration orders but seems to favor higher integration orders for nonlinear analysis. [1, 2] The likely reason is that lower integration orders can result in an assembled structure stiffness matrix that is singular or ill-conditioned. [3] However, it has been suggested that, in general, "it is best to use as low an order as possible without precipitating a numerical disaster". [4] The first analyses performed with Model 2

used higher integration orders and produced load vs. dent-depth responses that were very much stiffer than the experimental response. The subsequent use of reduced integration orders with this model resulted in a much improved agreement. This may be attributed to the fact that the resulting inaccuracies in the numerical integration may compensate for the inherent stiffness of the finite element solution. [3]

ADINA allows up to 4 integration points in the in-plane directions of the shell elements as well as through the thickness. The default values for the in-plane directions are 2 and 3 for the 9- and 16-node elements, respectively. [1] However, higher integration orders of 3 and 4 respectively are suggested. [2] Although it is suggested that a higher integration order through the thickness may be more effective for elasto-plastic analysis, no significant difference was noted in a comparison of 2 and 3 integration points through the thickness. For the sake of economy of computation, 2 point integration through the thickness was used thereafter. Tables 2 and 3 show the integration orders for the various models used in the analysis. A single integration point was used for the truss elements.

3.4.2 Solution of Equations

The Broyden-Fletcher-Goldfarb-Shanno (BFGS) method, which utilizes an updated stiffness matrix for the equilibrium iterations, was selected for solving the equilibrium equations rather than the modified Newton iteration. Due to its improved convergence characteristics, this is the method recommended when significant nonlinearities are expected. [1, 2] The convergence criteria were the default values in ADINA. Hence, only an energy convergence tolerance was used.

Although some attempts were made at smoothening the calculated response by tightening the convergence tolerances, greater success was obtained by reducing the load increments. This is likely due to the load-history dependence of the solution because of

the elasto-plastic material model used and the local unloading of the shell elements as a result of the redistribution of the load over the contact area with the increasing dent depth.

3.4.3 Development of Analytical Procedure

Specimen P1 was the first to be analyzed. The first analysis that produced a reasonable correlation between the calculated response and experimental data was by using Model 2. The use of reduced integration orders for the shell elements (2x2 in the in-plane directions for the 9-node shell elements) resulted in a significant reduction in the stiffness of the response and provided a much improved agreement with the experimental response as discussed in Sec. 3.4.1.

In order to more closely model the application of a distributed load over the relatively coarse mesh of Model 2 in the region of the indentation, a quad-linear stress-strain relationship for the truss elements was used. That is, two transitions between essentially zero and infinite modulus of elasticity were used causing each truss element to gradually stiffen as the indentation spread circumferentially from one nodal point to the next. However, the determination of the specific values of stress and strain for defining the stress-strain relationship of each truss element that would result in a reasonably smooth calculated response proved to be a tedious trial and error process requiring considerable effort.

Attempts to analyze the indentation of Specimen P2 with Model 2 were abandoned as it became apparent that the same trial and error process used to determine the stress-strain relationship for each truss element in the analysis of Specimen P1 would have to be repeated. Consequently, Model 4 with a much finer mesh in the dented area was developed which allowed the use of a single transition in the stress-strain relationships. (See Sec. 3.2.1).

Specimen IIICI was also analyzed with Model 4. For this case, it was found that use of higher integration orders (4x4 in the in-plane directions for the 16-node shell elements) gave slightly better agreement with the experimental data. However, due to the finer mesh of Model 4, the difference in the responses calculated with reduced and higher integration orders was not as significant as for Model 2.

Model 8 was used in the analysis of Specimens IBII and IIAII in order to accommodate their larger dent depths. Although this model produced results which correlated well with the experimental response, the slightly coarser mesh of Model 8 resulted in a slightly more erratic calculated response.

3.5 Results of Analysis

The load vs. dent depth relationships, calculated and experimental, are presented for comparison. The results are shown in non-dimensionalized form as defined in Section 2.2.2; the load as a fraction of the simple beam collapse load, and the dent depth as a percentage of the diameter. All pertinent information related to the analytical solutions, such as the specimen analyzed, number of load increments, integration order for the shell elements, and the finite element model used, is given in Table 3.

The load vs. dent depth relationship for Specimen P1 calculated with Model 2 and the experimental curve are shown in Fig. 17. The results of the analysis of Specimens P1 and P2 with Model 4 and their experimental curves are shown in Figs. 18 and 19. The analytical (Model 4) and experimental responses of Specimen IIICI are shown in Fig. 20 and of Specimens IBII and IIAII (Model 8) in Figures 21 and 22, respectively.

3.6 Computational Cost

The finite element analysis was performed on a Control Data Corporation Cyber 180 Model 850 computer running the NOS and NOS/VE operating systems. For the most part, the NOS/VE operating system was used because it was more economical. For two benchmark jobs run to compare costs under these two operating systems, the NOS/VE operating system showed a cost saving in CPU time of better than 40%.

The cost in terms of CPU time varied with each of the three models. It was also sharply dependent on the integration order used with the shell elements, but otherwise it was generally consistent in terms of CPU time per load step for each model. Computational times listed in Table 2 are representative for the runs made with each model. The times for each run varied considerably. At the high extreme, the CPU time per load increment for Model 8 with reduced integration orders averaged 57 seconds. With over 300 load increments used in the analysis of a dent depth equal to 10% of the diameter, this required several hours of CPU time for a single load-deformation relationship. More typically, 150 to 200 load increments were used with 12 to 36 CPU seconds per increment.

3.7 Discussion

The validity of the finite element analysis was verified by comparison of the calculated response with the experimental. For the two large-diameter, fabricated specimens, the correlation was not as good as for the smaller, manufactured specimens which had been stress relieved. Specifically, the calculated response was initially much stiffer than the experimental for the fabricated specimens as shown in Figs. 17, 18, and 19. An implication is that residual stresses, which are not taken into account in the finite element analysis, but are present in the fabricated specimens, reduce the denting resistance of the tube. An investigation of this effect is discussed in Chapter 4.

The effect of the number of integration points used in the calculation of the shell element stiffness matrices also seemed to have a significant effect on the responses calculated with Model 2. However, the effect of integration orders on the response calculated with Model 4, which has a much finer mesh, was not nearly as great. This observation supports the reasoning that the inaccuracy resulting from reduced integration orders may offset the excessive stiffness inherent in a coarse mesh (See Sec. 3.4.1).

Some observations may be made from the experiences described above. First, it is desirable to use a relatively fine mesh in the area of indentation (Compare Model 2 with Models 4 and 8). The added computational expense may be, at least partly, recovered by the use of reduced integration orders with the finer mesh. Additionally, the use of tri-linear stress-strain relationships for the truss elements also proved effective in conjunction with a finer mesh. Also, due to the high degree of non-linearity of the problem, it is necessary to use very small load increments. Lastly, an obvious conclusion is that considerable computational resources are required for finite element analysis of indentation of tubular members.

4. Effect of Residual Stresses

The much improved correlation between the results of the finite element analysis (which does not include consideration of residual stresses) and the experimental data on the manufactured, stress relieved specimens (Specimens IBII, IIAII, and IIICI) in comparison with the fabricated specimens (Specimens P1 and P2) prompted the investigation into the effect of residual stresses on the indentation behavior.

To gain an appreciation of the phenomenon, the formation of a circular ring from a straight bar was analyzed first since the resultant residual stresses are analogous to the rolling residual stresses in a fabricated tube. Then, the indentation of a tube was taken to be analogous to the flattening of a segment of the ring. The results of this analysis showed that the residual stresses had a significant reducing effect on the internal moment required to flatten a segment of the ring.

4.1 Residual Stresses in a Circular Ring

As a first step in determining the effect of residual stress on the indentation behavior, the magnitude and pattern of residual stresses in a ring resulting from cold-bending were determined. Considering the rectangular cross section to be elastic-perfectly plastic, the equation for the initial curvature, Φ_i, required to produce a ring with a final curvature Φ (equal to the reciprocal of the radius, $\frac{1}{R}$) is

$$\left(\frac{\Phi_i}{\Phi_y}\right)^3 - \left(\frac{3}{2} + \frac{t}{D\epsilon_y}\right)\left(\frac{\Phi_i}{\Phi_y}\right)^2 + \frac{1}{2} = 0 \qquad for\ \Phi \geq \Phi_y \tag{4.1}$$

where

t = the wall thickness

D = the diameter of the ring

ϵ_y = the yield strain of the material

Φ_y = the yield curvature = $\frac{2\epsilon_y}{t}$

An explicit approximation for Φ_i is readily obtained by assuming that the difference between the initial and final curvatures is equal to 1.5 times the yield curvature, i.e., $\Phi_i - \frac{1}{R} = 1.5\Phi_y$. This approximation is very good for values of $\frac{\Phi}{\Phi_y} \geq 2.0$ due to the asymptotic nature of the moment-curvature relationship for elastic-perfectly plastic materials. This lower bound for the approximation translates to $\frac{t}{D\epsilon_y} \geq 2.0$, which, even for moderately high strength steels, say $\epsilon_y \approx 0.0025$, is satisfied for $\frac{D}{t}$ ratios up to 200. With this approximation, which is valid for the range of $\frac{D}{t}$ ratios and yield strains typically encountered in offshore structures, Eq. (4.1) simplifies to

$$\frac{\Phi_i}{\Phi_y} = \frac{\Phi}{\Phi_y} + \frac{3}{2} \tag{4.2}$$

or, with $\Phi = \frac{1}{R}$,

$$\Phi_i = \frac{1}{R} + \frac{3\epsilon_y}{t} \tag{4.3}$$

which gives the maximum required curvature in terms of the thickness, yield strain, and the final radius, R. Since the final curvature is equal to $\frac{1}{R}$, and the linearly elastic relaxation curvature must be $\frac{3\epsilon_y}{t}$, the resulting residual stress distribution is as shown in Fig. 23. The maximum residual stress develops at distance αt from the mid-thickness, where

$$\alpha = \frac{D\epsilon_y}{2t} + 3\epsilon_y \tag{4.4}$$

and has the value of

$$\sigma_y(1 - 3\alpha) \tag{4.5}$$

The residual stress in the outer fiber is compressive and is equal to 1/2 the yield stress.

It should be noted that these residual stresses slightly deviate from self equilibrium due to the approximation made for Eqs. (4.2) and (4.3).

4.2 Effect of Residual Stresses in a Circular Ring

With the residual stress distribution for the cold-rolling process known, it is possible to determine the moment required to flatten (return to zero curvature) a segment of the ring by superimposing the stress distribution due to the change in curvature onto the residual stresses. The elastic moment required is directly proportional to the change in curvature. The results of this superposition are shown in Fig. 24.

A comparison of the stresses resulting from flattening a segment of a circular ring with and without residual stresses indicates that the moment in the flattened region is smaller when residual stresses are present. The reduction in moment calculated for a ring having the same radius, thickness and material properties as Specimen P1 was 21.1%, and 22.1% for P2.

Although these calculations are only an approximate attempt to quantify the effect of residual stresses due to cold-rolling plate into tubular members, they support the contention that residual stresses lead to a significant reduction in the load required to produce an indentation and in the energy dissipated in the process.

4.3 Limited Range of the Effect of Rolling Residual Stresses

The load vs. dent-depth relationships for the two fabricated specimens, P1 and P2, shown in Figs. 18 and 19 indicate that, in the initial stages of indentation, the response calculated by ADINA is much stiffer than the experimental response. However, beyond this initial range, the curves seem to approximately parallel each other.

The limited extent of the range for which the calculated response is stiffer than

the experimental response is a consequence of the local plastification and unloading that occur during deformation. This plastification and unloading have a mitigating effect on the cold-rolling residual stresses since this process results in the formation of its own residual stresses.

4.3.1 Plastification and Residual Stresses Due to Indentation

A simple model of the deformation of a cross section of a tube subjected to indentation is shown in Fig. 25. The indentation results in local plastification followed by unloading as the localized area of plastification (plastic hinge) migrates through a given point in the deformation process. As a result, residual stresses are formed in a manner similar to that resulting from cold-rolling during fabrication and have a similar effect. However, it appears from the comparison of the analytical and experimental results that the effect is not realized until some finite deformation takes place.

Wierzbicki and Suh presented a method for analyzing the denting of tubes under combined loading. [17] Their method involves the analysis of a simplified shell model consisting of a series of rings and longitudinal strips. The deformation assumed for the ring elements is used here to show that the effect of residual stresses due to cold-rolling is mitigated in the deformation process. A deformed ring was assumed to be divided into four segments of constant curvature separated by moving plastic hinges as shown in Fig. 26. Although this deformation is not consistent with indentation due to lateral loading since adjacent segments have constant curvatures of opposite sign, it does approximate the observed deformations.

The shape of the deformed ring for a given dent depth, d, is a function of three parameters, R_1, R_2, and θ defined in Fig. 26. From the assumed geometry and the assumption of inextensibility of the ring in the circumferential direction, the following two equations are obtained:

$$R_1\theta + R_2(\pi-\theta) + (R_1-R_2)\sin\theta = \pi R \tag{4.6}$$

$$d = 2R - \{R_1(1-\cos\theta) + R_2(1+\cos\theta)\} \tag{4.7}$$

Since one more equation is needed to define the assumed geometry in terms of the dent depth, the following relationship was suggested:

$$R_2 = \left(\frac{\theta}{\theta_0}\right)^n R \tag{4.8}$$

Wierzbicki and Suh further suggest that n=1 and that θ_0, the initial value of θ (undeformed geometry), be set to $\frac{\pi}{2}$ resulting in the relationship

$$R_2 = \frac{2\theta}{\pi} R \tag{4.9}$$

With this assumed deformation field, the curvature of the segments adjacent to the flattened portion of the ring increases since R_2 decreases with an increasing dent depth. Plastification ensues as the curvature in these segments increases beyond the yield curvature $\left(\frac{1}{R_2} - \frac{1}{R} > \Phi_y\right)$. As the deformation increases, the hinges adjacent to the flattened segment migrate apart, resulting in a reversal of curvature from one side of the hinge to the other. If plastification has occurred in the segments with radius R_2, the moment required for this reversal in curvature is reduced. The condition for incipient plastification is given by

$$r_2 > \frac{t}{D\epsilon_y + t} \tag{4.10}$$

where

$$r_2 = \frac{R_2}{R} \tag{4.11}$$

This local plastification, followed by a reversal in curvature, is analogous to cold-rolling and subsequent flattening (denting). The relative dent depth at which plastification is initiated is determined from Eqs. (4.6), (4.7) and (4.9) and is given by

$$\frac{d}{D} = 1 - \left[\frac{\pi (1 - r_2) + r_2(\theta + \sin\theta)}{2 (\theta + \sin\theta)} (1 - \cos\theta) + \frac{r_2}{2} (1 + \cos\theta) \right] \tag{4.12}$$

The solution of Eqs. (4.10) and (4.12) for the dent depths at which plastification initiates in Specimens P1 and P2 gives the relative dent depths of 6.1% and 10.3%, respectively. This indicates that the residual stresses due to denting deformation would have no effect until these dent depths are reached. However, these calculated values of the dent depth are obviously dependent on the assumptions made for the deformed shape.

4.3.2 Assumed and Observed Deformations

The calculated relative dent depth at which the effect of residual stresses is mitigated by plastification during deformation is higher than is indicated by the comparison of the analytical and experimental load vs. dent depth curves (Figs. 18 and 19). This is apparently due to the assumed deformation geometry used in the calculations.

Although Wierzbicki and Suh based their assumed deformation on observation of some test specimens and certain analytical considerations, the deformations of Specimens P1 and P2 differed somewhat from this assumed geometry. The actual deformations of P1 and P2 more closely resembled the geometry shown in Fig. 3 rather than the cross-sectional geometry of Wierzbicki and Suh's model shown in Fig. 26. This is likely due to the relatively high D/t ratios of these two specimens. A deformation model of a ring with migrating plastic hinges based on the geometry shown in Section A-A of Fig. 3 is shown in Fig. 25. The two plastic hinges migrate apart as the dent depth and the length of the flattened segment of the ring increase. The effect of the formation of a plastic hinge followed by a reversal in curvature (flattening), as the plastic hinges migrate, is the same as discussed in Sec. 4.3.1.

According to this deformation model, the formation of the migrating plastic hinges occurs at infinitesimal dent depth. This implies that the effect of residual stresses due to cold rolling would be immediately nullified. Thus, this model obviously does not reflect the actual deformation process but does provide a qualitative indication that the dent depths calculated in Sec. 4.3.1 should be greater than the actual values obtained. Hence, the dent depth at which the effect of residual stresses becomes insignificant in the deformation process is somewhat less than calculated from Eqs. (4.10) and (4.12), especially for tubes with large D/t ratios.

5. Approximation of Denting Behavior

An approximate method for predicting the load vs. dent-depth response of tubular members has been developed on the basis of a multi-variable regression analysis of the experimental data reported in Ref. [14]. Application of the method is limited to the domain of the experimental data but can readily be expanded as more data is incorporated. A general description of the regression analysis used to determine the approximating function and a discussion of its application to the denting analysis of tubulars are given in the following sections.

5.1 Regression Analysis

The multi-variable regression analysis employed is the method described by Ostapenko and Surahman and used by them to develop axial load vs. axial deformation relationships of plates and stiffened plates in the pre- and post-ultimate ranges. [9] The procedure involves selection of an approximating function on the basis of an expected analytical relationship or a qualitative study of the data. The coefficients of each term of the approximating function are then determined by minimizing the sum of the squares of the error at each point.

For example, for the case of a single independent variable, x, the approximating function, $\bar{f}$, can be expressed as a series of m terms,

$$\bar{f} = \sum_{i=1}^{m} a_i h_i(x) \tag{5.1}$$

where h_i are linearly independent functions of the independent variable, x, and the a_i are the coefficients to be determined. This approximation can be equivalently expressed as the product of two matrices

$$\bar{f} = H A \tag{5.2}$$

where H is a row matrix of m h_i functions of the independent variable and A is a column matrix of the a_i coefficients. Matrix H is called the *coordinate function* for the independent variable, x, and qualitatively reflects the relationship between the dependent and independent variables.

When there are more than one independent variables, a coordinate function for each independent variable is needed. Each coordinate function is selected to reflect the relationship between the dependent variable and a particular independent variable while all others are held constant. The approximating function for the multivariable relationship is then given by Eq. (5.2) except that matrix H is obtained by combining the coordinate functions of individual independent variables as a *direct product*. [9] The *direct product* operation is illustrated by considering the following example for two independent variables. If the two individual *coordinate functions* are $\mathrm{H1} = [\,h_{11}\ h_{12}\,]$ and $\mathrm{H2} = [\,h_{21}\ h_{22}\ h_{23}\,]$, then, their *direct product*, with $2 \times 3 = 6$ terms, is given by

$$\mathrm{H} = \mathrm{dir}(\mathrm{H1}, \mathrm{H2}) = [h_{11}h_{21} \quad h_{12}h_{21} \quad h_{11}h_{22} \quad h_{12}h_{22} \quad h_{11}h_{23} \quad h_{12}h_{23}] \tag{5.3}$$

Note the sequence of multiplication adopted in this definition.

More generally, for a relationship with k independent variables, the coordinate functions would be designated $\mathrm{H1} = [\,h_{11}\ h_{12}\ \cdots\ h_{1m_1}]$, $\mathrm{H2} = [\,h_{21}\ h_{22}\ \cdots\ h_{2m_2}]$, and $\mathrm{Hk} = [\,h_{k1}\ h_{k2}\ \cdots\ h_{km_k}]$. The direct product is then given by

$$\begin{aligned}\mathrm{H} = \mathrm{dir}(\mathrm{H1}, \mathrm{H2}, \ldots, \mathrm{Hk}) = [&h_{11}h_{21}\ldots h_{k1} \quad h_{12}h_{21}\ldots h_{k1} \quad \cdots \quad h_{1m_1}h_{21}\ldots h_{k1} \\ &\cdots \quad h_{11}h_{22}\ldots h_{k1} \quad \cdots \quad h_{1m_1}h_{2m_2}\ldots h_{km_k}]\end{aligned} \tag{5.4}$$

and it contains m elements, $m = \prod_{i=1}^{k} m_i$.

Once the elements of H are established, the coefficients, A, are determined from a given set of numerical data by minimizing the sum of the squares of the errors at each data point. This procedure can be succinctly presented in matrix form. Consider a

set of data of n points with the given values of the dependent variable listed in a column matrix, F. The corresponding values of the approximating function, $\overline{F}$, are then given by

$$\overline{F} = B\,A \tag{5.5}$$

where B is a (n,m) rectangular matrix each j^{th} row of which is equivalent to the row matrix, H, evaluated at the values of the independent variables corresponding to the j^{th} element of F. As before, A is a (m,1) column matrix of the yet unknown coefficients.

The errors between the approximating function and the given data at each point are then

$$\overline{F} - F = B\,A - F \tag{5.6}$$

The sum of the squares of the errors, the "error function", is

$$E = (B\,A - F)^T\,(B\,A - F) \tag{5.7}$$

or, in an expanded form,

$$E = A^T B^T B A - 2F^T B A + F^T F \tag{5.8}$$

Minimization of the error function by setting its first derivative with respect to each element of A equal to zero results in the following simultaneous equations:

$$V\,A = Q \tag{5.9}$$

where

$$V = B^T B \tag{5.10}$$

and

$$Q = B^T F \tag{5.11}$$

This system of linear equations is then solved for coefficients A.

This method has characteristics which can be taken advantage of in developing an algorithm for a computer program. One of these is that the elements of matrix V can be generated by successively evaluating each row of matrix B and computing its contributions to the elements of V without having the other rows of B in memory. Consequently, the memory requirements for the execution of the program are not dependent on the number of data points but only on the number of terms of the approximating function, H. Furthermore, matrix V is symmetrical, hence less memory is required and a more efficient algorithm for solving the simultaneous equations can be used.

Also, in the absence of a clearcut relationship between the dependent and independent variables, it is unlikely that a "first guess" at the coordinate functions will result in the best fit of the approximating function to the given data. Thus, it is usually desirable to vary the composition of the individual coordinate functions in order to improve the correlation. This is facilitated by simply defining the coordinate functions in separate program units which can readily be interchanged in the program. Then, after performing the regression analysis, the "goodness" of fit for a given set of coordinate functions can be determined by evaluating the root-mean-square of the errors or other measure of the total error, and the most suitable set selected.

5.2 Elimination of Independent Variables

Once the regression analysis has been completed, it may be desirable to establish the approximating function with one or more of the independent variables set to a predetermined constant value. For example in the current study, the relationships between the load and dent-depth were of interest for constant values of member geometry and material properties. In other cases, it may simply be desirable to eliminate a single variable from the final approximating function. In the study by Ostapenko and Surahman on the axial response of plates, the effects of initial imperfections were in-

cluded in the regression analysis but in the final approximation this variable was set to a constant value determined from allowable or expected imperfections in plates. [9] This procedure has also been proven useful in studying the effects of individual variables and of the composition of their coordinate functions on the accuracy of the approximating function.

In the process of eliminating a variable by assigning it a constant value, the number of terms in the approximating function is reduced by a factor equal to the number of terms in the coordinate function for that particular variable. The coefficients for this shortened approximating function are readily calculated from the set of coefficients of the complete approximating function. Thus, there is no need to perform the regression analysis again. The mechanics of this procedure for the elimination of a single variable are indicated in the following paragraphs.

In order to modify the approximating function for a preset value of the i^{th} independent variable, the elements of A are arranged into a (m^*,m_i) rectangular matrix, A^*, where m_i is the number of terms of the i^{th} coordinate function, Hi, and $m^* = m \div m_i$. The rearrangement is performed so that each j^{th} column of A^* contains only the elements of A which are coefficients of the approximating function containing the j^{th} term of the coordinate function, Hi. The reduced matrix of coefficients, A_r, is then given by

$$A_r = A^* Hi^T \tag{5.12}$$

where the elements of Hi are evaluated at the preset constant value. The approximating function is then

$$\bar{f} = H_r A_r \tag{5.13}$$

where the elements of H_r are the unique elements of H remaining after the elimination

of the terms containing elements of Hi. Note that Eq. (5.13) is equivalent in form to Eq. (5.2).

The elimination of more than one variable can be accomplished in one of two ways. One method is to succesively apply the above procedure and eliminate the variables one at a time. Or alternatively, when the coordinate functions for the variables to be eliminated appear as consecutive terms in the direct product operation defining the approximating function, these variables may be eliminated en masse. This is accomplished by replacing the single coordinate function, Hi, in Eq. (5.12) by the direct product of the coordinate functions whose variables are to be eliminated and making the appropriate arrangement of the A^* matrix. For example, to eliminate the 2^{nd}, 3^{rd}, and 4^{th} variables in one operation, the equivalent of Eq. (5.12) would be

$$A_r = A^* (\mathrm{dir}(\, H2, H3, H4\,))^T \tag{5.14}$$

The determination of A_r and the elimination of elements from H to form H_r is demonstrated in the following section where this procedure is applied to define the load vs. dent-depth relationship for given material properties and geometry.

5.3 Regression Analysis of Load vs. Dent Depth Data

Before performing the regresion analysis of the load vs. dent-depth data from Ref. [14], it was necessary to first determine the number and the form of the variables needed to describe the denting behavior. The coordinate functions were then selected to define the relationship between these variables.

5.3.1 Determination of Variables

The problem was to find a set of variables which, while incorporating all the pertinent parameters, would represent the given data in a relatively smooth pattern with a minimun of scatter and permit the use of an approximating function with a minimum number of terms. The search for these variables proved to be the most difficult and time-consuming phase of the analysis.

The first step in the process was to identify all the parameters associated with the load-deformation relationship. Load, dent-depth, tube diameter, wall thickness, and yield stress of the material, were obvious. The modulus of elasticity was also included as a non-dimensionalizing factor although it was constant for the data analyzed. Due to the boundary conditions imposed during indentation of the test specimens as described in Appendix A, the length of the specimen was not considered as a variable in the analysis, nor was the dent geometry since all of the specimens were subjected to a "knife edge" loading.

The next step was to combine the parameters into non-dimensionalized quantities. Obviously, a load variable (the dependent variable) and a deformation variable were needed, as well as, a third and perhaps a fourth variable to represent the effects of member geometry and material properties. Since various non-dimensionalized forms were possible for each variable and the relationship between the variables was unclear in the absence of a closed analytical solution for the denting behavior, a trial and error approach had to be used. The initial attempts simply involved plotting various non-dimensionalized forms of the denting load vs. the dent-depth to diameter ratio for test specimens with the same $\frac{D}{t}$ ratio and studying the effect of the yield stress on the relationship. After many trials with various forms of the variables and qualitative appraisal of the plots of the data, three variables were selected which seemed to represent the data by a relatively smooth surface. These were the following:

The load variable, Q (the dependent variable)

$$Q = \frac{P}{D^2 \sigma_y} \tag{5.15}$$

the deformation (dent depth) variable, W

$$W = \frac{d\,E}{D\,\sigma_y} \tag{5.16}$$

and the member geometry variable, B

$$B = \left(\frac{D}{t}\right)^2 \frac{E}{\sigma_y} \tag{5.17}$$

5.3.2 Selection of Coordinate Functions

Once the dependent and independent variables had been established, the next step before performing the regression analysis was the selection of coordinate funtions for each of the independent variables. The object of this task was to select the individual terms of the coordinate function so that the "best fit" could be achieved with the fewest terms. For this step, the dependent variable, Q, was plotted versus each independent variable for some constant values of the remaining variable. The terms of the coordinate function were then selected from a qualitative appraisal of the plot of the relationship between the dependent variable, Q and the corresponding independent variable. For example, a typical load-deformation curve (Q vs. W) for a constant value of B is shown in Fig. 28. The shape of this curve suggests a square or cube root relationship. It is also evident that a constant term is not needed since the curve will always pass through the origin. Likewise, a plot of a typical Q vs. B relationship shown in Fig. 29 suggests an inverse relationship. These considerations led to the selection of the general form of the two coordinate functions.

After examining the relationships between the variables and establishing a set of coordinate functions, the regression analysis was performed with the given data. In an

attempt to improve the approximation, the regression analysis was repeated with variations of the coordinate functions. The two coordinate functions that resulted in the best approximation (smallest root-mean-square of the errors) and yet had a small number of terms were

$$\mathrm{H1} = [\, W^{0.5}(10)^{-3} \quad W(10)^{-4} \quad W^2(10)^{-5} \,] \tag{5.18}$$

and

$$\mathrm{H2} = [\, (10)^{-2} \quad B(10)^{-8} \quad B^{-1}(10)^4 \quad B^{-2}(10)^{10} \,] \tag{5.19}$$

The multipliers of ten were included only to make the coefficients, A, have approximately the same order of magnitude.

The direct product of these two matrices, H1 and H2, produces the row matrix H which contains twelve elements and has the form

$$\mathrm{dir}(\mathrm{H1}, \mathrm{H2}) = [h_{11}h_{21} \quad h_{12}h_{21} \quad h_{13}h_{21} \quad h_{11}h_{22} \quad \cdots \quad h_{13}h_{24}]$$

and is given by

$$\begin{aligned} \mathrm{dir}(\mathrm{H1}, \mathrm{H2}) = [\, & W^{0.5}(10)^{-5} \quad W(10)^{-6} \quad W^2(10)^{-7} \quad W^{0.5}B(10)^{-11} \\ & WB(10)^{-12} \quad W^2B(10)^{-13} \quad W^{0.5}B^{-1}(10) \quad WB^{-1} \\ & W^2B^{-1}(10)^{-1} \quad W^{0.5}B^{-2}(10)^7 \quad WB^{-2}(10)^6 \quad W^2B^{-2}(10)^5 \,] \end{aligned} \tag{5.20}$$

The regression analysis resulted in the following set of twelve coefficients, $\mathrm{A}^T = [\, a_1 \;\; a_2 \;\; a_3 \;\; \cdots \;\; a_{12} \,]$

$$\begin{aligned} \mathrm{A}^{\mathrm{T}} = [\, & -61.262 \quad -3.403 \quad 4.102 \quad 16.733 \quad -7.557 \quad -0.3549 \\ & 79.630 \quad 169.67 \quad -12.778 \quad 15.909 \quad -136.78 \quad 9.527 \,] \end{aligned} \tag{5.21}$$

5.3.3 Reduction to One Independent Variable

By assigning the member geometry variable, B, a constant value, the load variable can be defined as a function of the deformation variable, W, only. This is accomplished by first rearranging A into the A^* matrix so that each j^{th} column contains only the coefficients of the j^{th} term of the coordinate function H2 (coordinate function for B).

$$A^* = \begin{bmatrix} a_1 & a_4 & a_7 & a_{10} \\ a_2 & a_5 & a_8 & a_{11} \\ a_3 & a_6 & a_9 & a_{12} \end{bmatrix} = \begin{bmatrix} -61.262 & 16.733 & 79.630 & 15.909 \\ -3.403 & -7.557 & 169.67 & -136.78 \\ 4.102 & -0.3549 & -12.778 & 9.527 \end{bmatrix} \quad (5.22)$$

Post-multplication of A^* by $H2^T$ evaluated for a given value of B results in a new set of constants, A_r (see Eq. (5.12)). Note that in this case A^* is a (3,4) matrix, $H2^T$ is a (4,1) matrix, and A_r becomes a (3,1) matrix. The approximate load vs. dent-depth relationship for a particular value of B now becomes

$$Q = H1\, A_r \quad (5.23)$$

Thus, the approximate load vs. dent depth relationship is now given by a three-term polynomial for a given yield stress, modulus of elasticity, and $\frac{D}{t}$ ratio.

As an example, the approximate load vs. dent-depth response is calculated for Specimen IIICI, for which a finite element analysis of the load vs. dent-depth relationship was also performed. For this specimen, from the data listed in Table 1, $B = 0.7513(10)^6$ and the coordinate function for B from Eq. (5.19) is

$$H2 = \begin{bmatrix} 0.01 & 0.007513 & 0.01331 & 0.01772 \end{bmatrix}$$

From Eq. (5.12), the A_r matrix is then

$$A_r = \begin{bmatrix} -61.262 & 16.733 & 79.630 & 15.909 \\ -3.403 & -7.557 & 169.67 & -136.78 \\ 4.102 & -0.3549 & -12.778 & 9.527 \end{bmatrix} \begin{bmatrix} 0.01000 \\ 0.007513 \\ 0.01331 \\ 0.01772 \end{bmatrix} = \begin{bmatrix} 0.8549 \\ 0.2559 \\ -0.03707 \end{bmatrix} \tag{5.24}$$

From Eq. (5.23), the approximate load vs. dent-depth relationship for Specimen IIICI is given by

$$Q = 0.8549\, W^{0.5}(10)^{-3} + 0.2559\, W(10)^{-4} + (-0.03707)\, W^{2}(10)^{-5} \tag{5.25}$$

A plot of this relationship (Eq. (5.25)) together with the experimental and the finite element analysis is shown in Fig. 30.

The approximate and experimental load vs. dent-depth responses for four additional specimens are shown in Fig. 31. These four specimens are representative of the 24 specimens used in the development of the approximate method, and include examples of the best and worst agreement between the experimental and approximate results. It should be noted that, since an approximation is based on all test curves, the deviation for a particular specimen may result not only from a limitation of the approximating function but also from the experimental variability (scatter of the data).

Since, as illustrated in Figs. 30 and 31, the approximating function agrees reasonably well with tests and finite element solutions, it can be recommended as an inexpensive and expedient tool for estimating the load vs. dent-depth behavior of tubular members.

5.4 Range of Applicability

The prediction of the load-deformation response is based on a limited set of experimental data consisting of only the load vs. dent depth relationships reported in Reference [14]. The approximating function and its coefficients were developed from this empirical data and therefore, caution should be exercised in extending the application beyond the range of member geometries and boundary conditions as follows

- $\frac{D}{t}$ ratios ranging from 40 to 60
- Yield stresses ranging from 200 MPa (30 ksi) to 500 MPa (70 ksi)
- "Knife edge" loading

Although the method has been developed from a limited database, it is hoped that more data would be included in the future and its range of applicability extended. This would include different modes of loading and a broader range of D/t ratios. The regression analysis can be readily performed on an expanded database and, if necessary, more independent variables may be incorporated. One of these may be a variable(s) to account for the effect of different dent geometries.

6. Summary, Conclusions and Recommendations

6.1 Introduction and Scope

The investigation of the indentation behavior of tubular members reported here consisted of experimental and analytical phases.

The experimental phase of the project provided data on the indentation behavior and energy dissipation of two large-diameter fabricated tubular specimens. These data together with the results of three tests conducted by others were compared with the results of the analytical work.

The analytical phase of the project consisted of a finite element analysis of the indentation problem and the development of an approximate method for predicting load vs. dent-depth response. The program ADINA was used for the finite element analysis because of its capability for performing large displacement materially nonlinear analysis. Some innovative modeling techniques were employed to simulate the contact of a rigid indenter with the tube wall. The approximate method developed was based on a regression analysis of empirical data.

6.2 Experimental Work

An indentation was introduced into two large-diameter, fabricated tubular specimens by the application of a lateral load through a rigid indenter. The load vs. deformation response during indentation was used to calculate the energy absorption as a function of the dent depth. Both specimens exhibited similar characteristics in this regard. (These specimens were subsequently subjected to axial load tests. [10, 11])

6.3 Analytical Work

The finite element analysis of the indentation of the test specimens was performed with the ADINA computer program which has the capability for material and geometric nonlinearities. To further assess the validity of the finite element modeling over a broader range of tube geometries and materials, the analysis was extended to include the indentation of three additional specimens from Reference [14]. In contrast to the two fabricated test specimens of the current program, these small-scale specimens were manufactured stress relieved tubes.

The finite element model consisted of an assemblage of shell elements to model the tube and a set of truss elements to simulate the application of a lateral load through a rigid indenter. Due to the high degree of nonlinearity inherent in the problem as a result of large deformations, plastification, and the nature of the loading, the incremental analysis had to be performed with a large number of load steps.

The correlation of the analytical and experimental results was significantly better for the manufactured stress relieved specimens than for the fabricated specimens. This prompted an investigation of the effect of residual stresses caused by cold-rolling. The results of the investigation confirmed the discrepancies in the behavior of the fabricated and manufactured specimens.

A simplified analytical method was developed for predicting the load vs. dent depth response of a tube subjected to lateral loading with a rigid indenter. The method was based on a regression analysis of the experimental data reported in Ref. [14]. The result of the analysis is a simple approximating function for the load-deformation relationship. Application of the method should, however, be limited to situations where the boundary conditions and material and geometric parameters do not deviate significantly from those in the database.

6.4 Conclusions

The finite element method, specifically, the commercially available general analysis programs, can be used for predicting the elastic-plastic large-deformation response of tubular members subjected to concentrated lateral loads.

However, the finite element analysis of a nonlinear system is not always a well defined or direct process. The modeling of the physical problem may not be straightforward; it may require innovative techniques or may only be an approximation due to the limitations of the computer program. Both of these situations were encountered in the analytical work in modeling the contact with a rigid indenter. Furthermore, several other factors can affect the results of the analysis. These can be the types of elements used and the discretization of the model to variations in the way the governing equations are formed and solved within the program. To determine the effect of these factors on the results, the analyst may have no alternative other than to perform further analyses with a rediscretized mesh or modified computational parameters. Obviously, this can be an expensive process, both in terms of time and computational resources.

Further limitations to the application of finite element programs is their requirements for the expertise typically needed to perform a non-linear analysis. The generation of a solution is usually expensive and should usually be correlated with experimental results or another analytical solution. This is especially true for non-linear analysis and when factors such as residual stresses may have an effect.

In view of the above considerations and of the results of this investigation, acceptance of the analysis should be contingent on an investigation of the ramifications of the modeling and the assumptions made in the analysis. Ideally, the analyst should have some empirical evidence with which to correlate the solution. Specifically, the

results of this investigation indicate that the indentation behavior of full scale fabricated tubular members may vary significantly from the behavior predicted by a finite element analysis. This is due, at least in part, to residual stresses in the fabricated members.

Since it has been shown that residual stresses can have a fairly significant effect on the indentation response, careful consideration should also be given to the accuracy of the experimental results obtained from stress relieved specimens for the prediction of the behavior of fabricated structures.

The regression analysis resulted in an approximate method for predicting load-deformation response for the indentation of tubular members. This simplified method, which could easily be implemented in a personal computer or programable calculator, provides a means of readily estimating the dent depth of a laterally loaded member.

6.5 Recommendations for Future Work

In order to develop a more complete understanding of the indentation behavior of tubular members as it relates to damage/energy dissipation in offshore structures, further research is needed. Experimental work, particularly full-scale testing of fabricated members is suggested in conjunction with analytical methods. Further work is needed to quantify the effects of a number of parameters. Among these are the dent geometry (geometry of the indenter), member length and end restraint conditions as well as the rate of loading. The effect of member loads (axial and flexural) on the denting behavior of tubular members should be investigated since collision or impact damage is likely to occur to a member in service. An effort should also be made to quantify the effects of residual stresses or possibly incorporate them into the analytical methods.

As more data (analytical and experimental) is generated, it should be included in the database. With additional variables incorporated into the regression analysis, the range of applicability of the approximate method could be extended, resulting in a more general approximation of the load vs. dent depth relationship.

Acknowledgments

This research was sponsored by the Minerals Management Service of the U.S. Department of the Interior (Contract No. 14-12-0001-30288) and the American Iron and Steel Institute (AISI Project 338) under the DOI/AISI Cooperative Research Program. The authors are grateful for this support and for the advice and guidance given by the members of the project Task Force; C.E. Smith and A.C. Kuentz, the respective representatives of the sponsoring institutions, and R.H. Wildt (Chairman of the Task Force) of Bethlehem Steel Corporation, C. Capanoglu of Earl and Wright, C.D. Miller of CBI Industries, Inc., J. de Oliveira of Conoco, Inc., and J.B. Gregory of the Minerals Management Service of the U.S. Department of the Interior. The authors also wish to thank Jon Taby of the Norwegian Institute of Technology for his generosity in providing information from research conducted at his institution.

Tables

Table 1: Specimen Data

Spec. No.	F_{ys}	Dimensions					Dent Depth	
		OD	t	L	D/t	L/r	d	d/D
	(MPa)	(m)	(mm)	(m)			(mm)	(%)
P1	203.8	1.02	6.73	2.44	150.7	6.80	28	2.7
P2	203.8	1.53	6.73	2.13	226.5	3.96	85	5.5
IBII	230	0.125	2.51	3.5	49.9	79.1	12.5	10.0
IIAII	351	0.161	2.52	3.5	63.6	61.8	16.1	10.0
IIICI	472	0.250	6.02	3.5	41.6	39.5	12.6	5.0
	(ksi)	(in.)	(in.)	(in.)			(in.)	(%)
P1	29.56	40.2	0.265	96.0	150.7	6.80	1.1	2.7
P2	29.56	60.3	0.265	84.0	226.5	3.96	3.3	5.5
IBII	33.4	4.93	0.099	138	49.9	79.1	0.492	10.0
IIAII	50.9	6.31	0.099	138	63.6	61.8	0.633	10.0
IIICI	68.5	9.86	0.237	138	41.6	39.5	0.496	5.0

Table 2: Computational Cost

Model	Integration Order of Shell Element		CPU time/Load Step (sec.)
	In-Plane	Through Thickness	
2	2	3	16
2	2	2	12
2	3	3	27
4	3	2	36
4	4	2	66
8	3	2	57

Table 3: Details of Analytical Models

Spec.	Analytical Model No.	Shell Element Integration Order	Number of Load Increments	Load vs. Dent Depth Response
P1	2	2x2x3	144	Fig. 17
P1	4	3x3x2	144	Fig. 18
P2	4	3x3x2	172	Fig. 19
IIICI	4	4x4x2	172	Fig. 20
IBII	8	3x3x2	332	Fig. 21
IIAII	8	3x3x2	302	Fig. 22

Figures

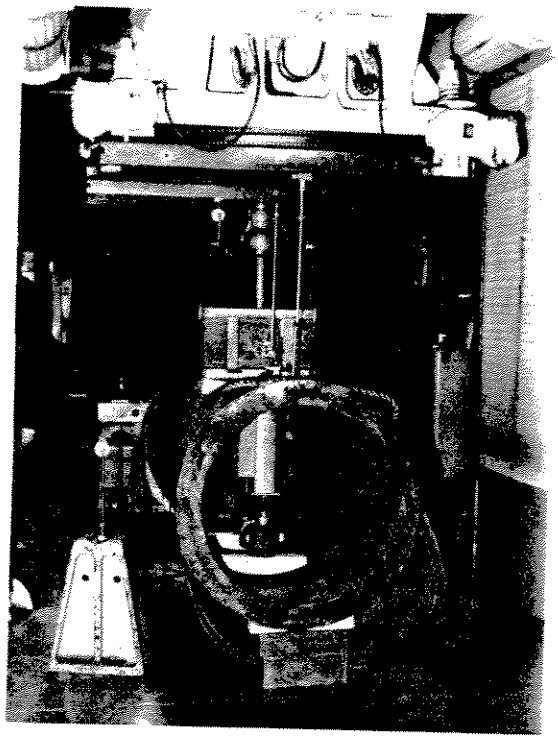

Figure 1: Set-up for Indentation of Specimen P1

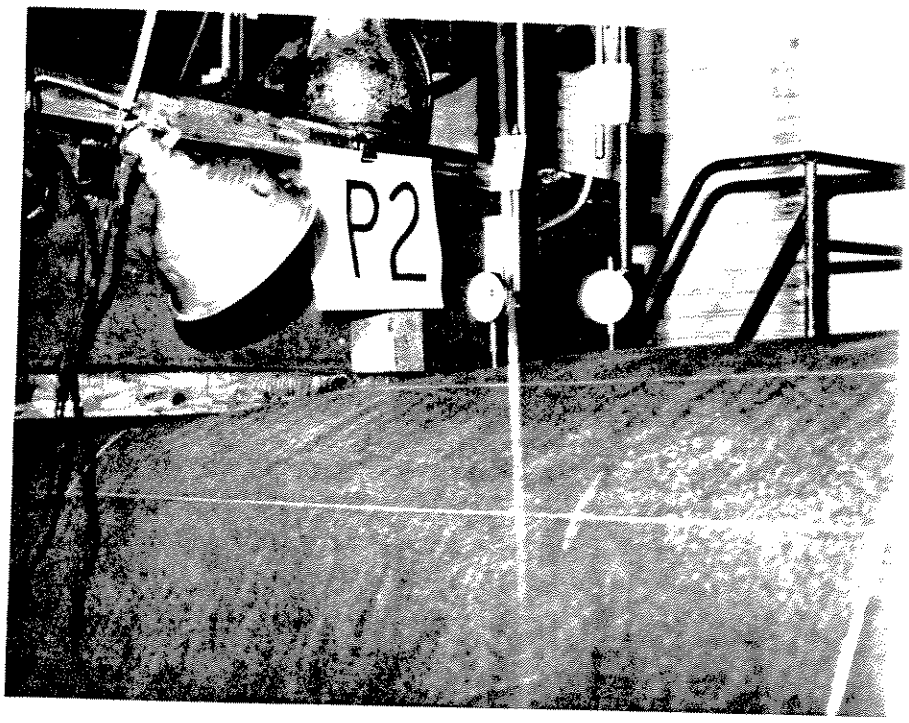

Figure 2: Indentation of Specimen P2

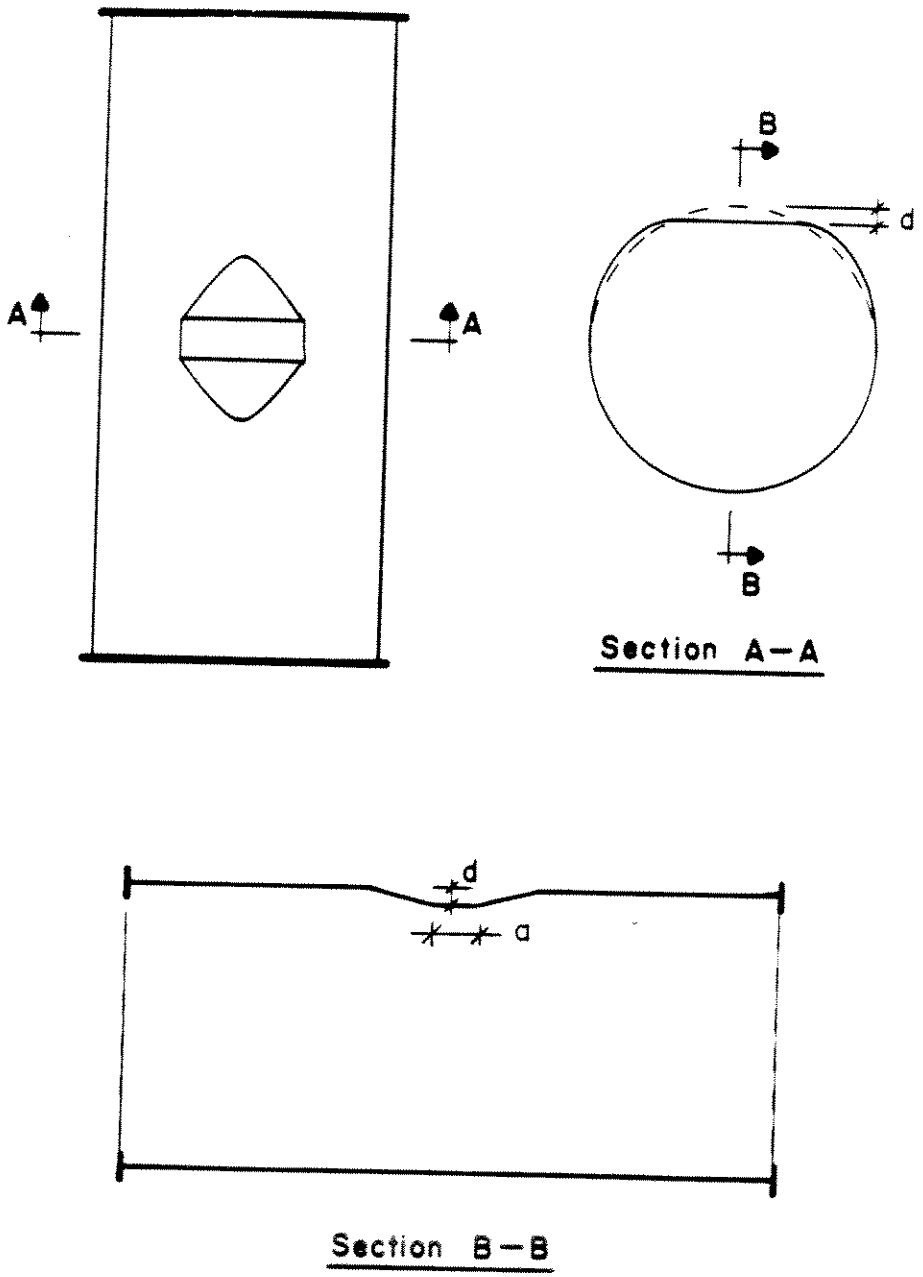

Figure 3: Schematic Representation of Ideal Dent Geometry

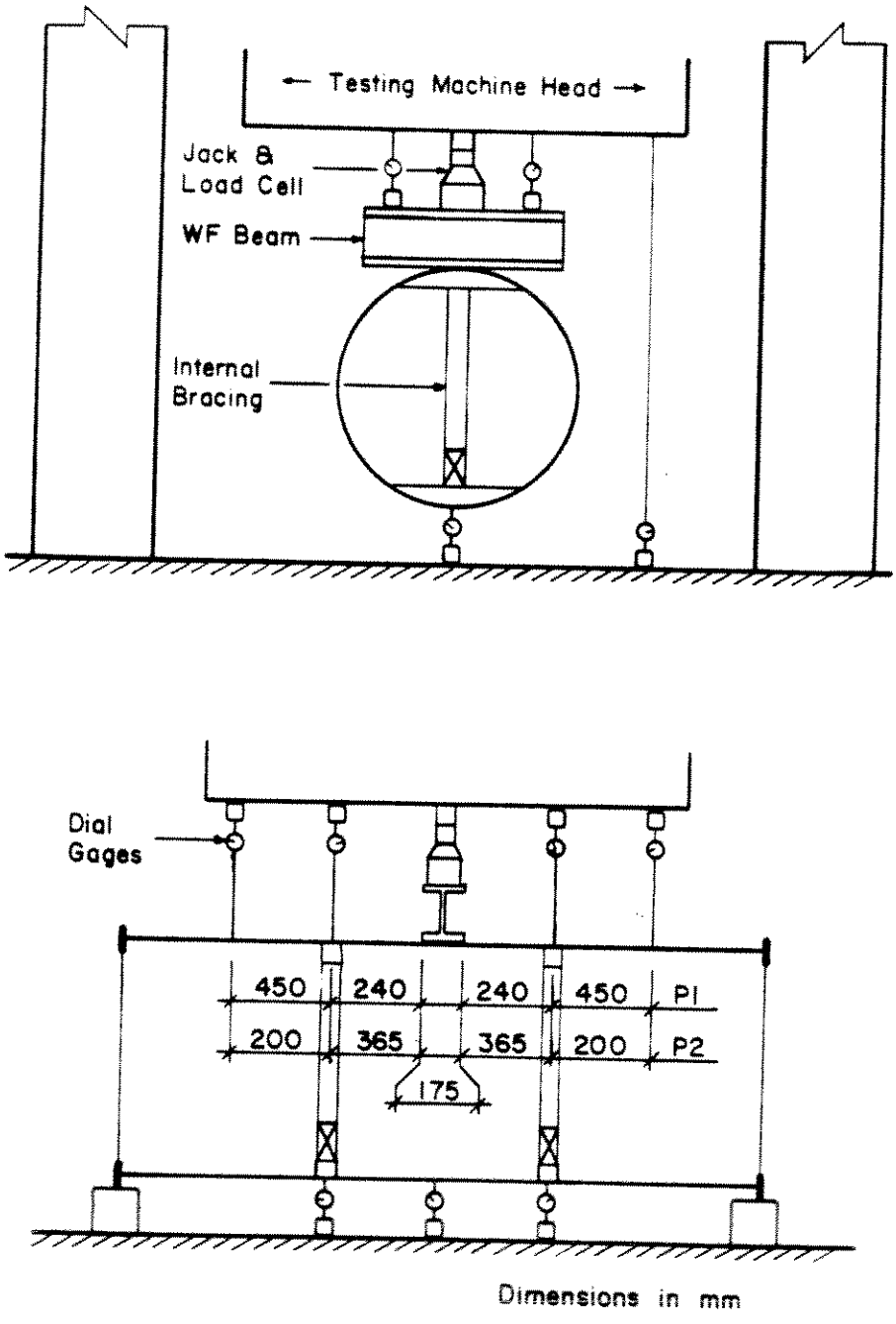

Figure 4: Schematic Representation of Test Set-up for Indentation

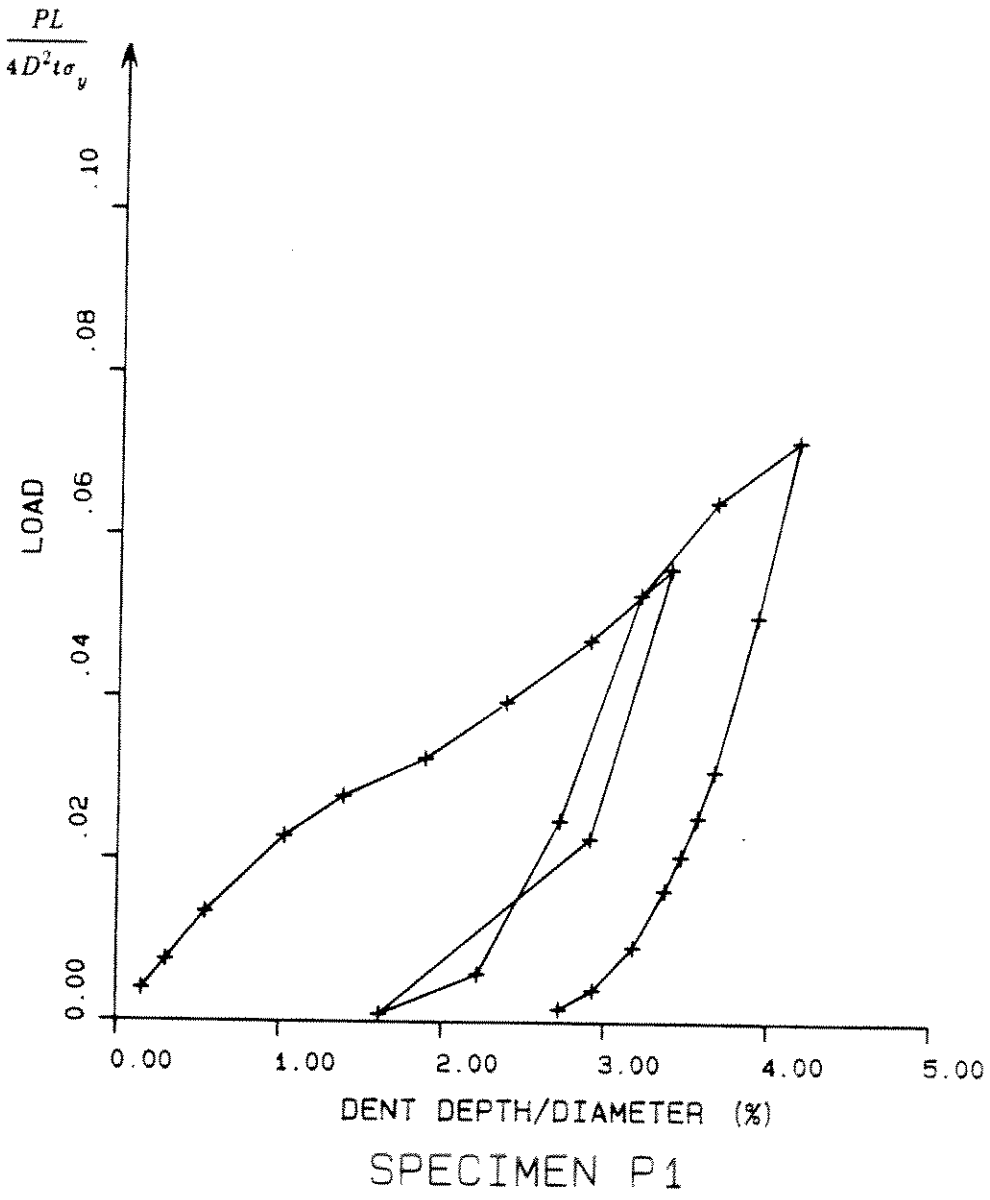

Figure 5: Experimental Load vs. Dent Depth Curve for Specimen P1

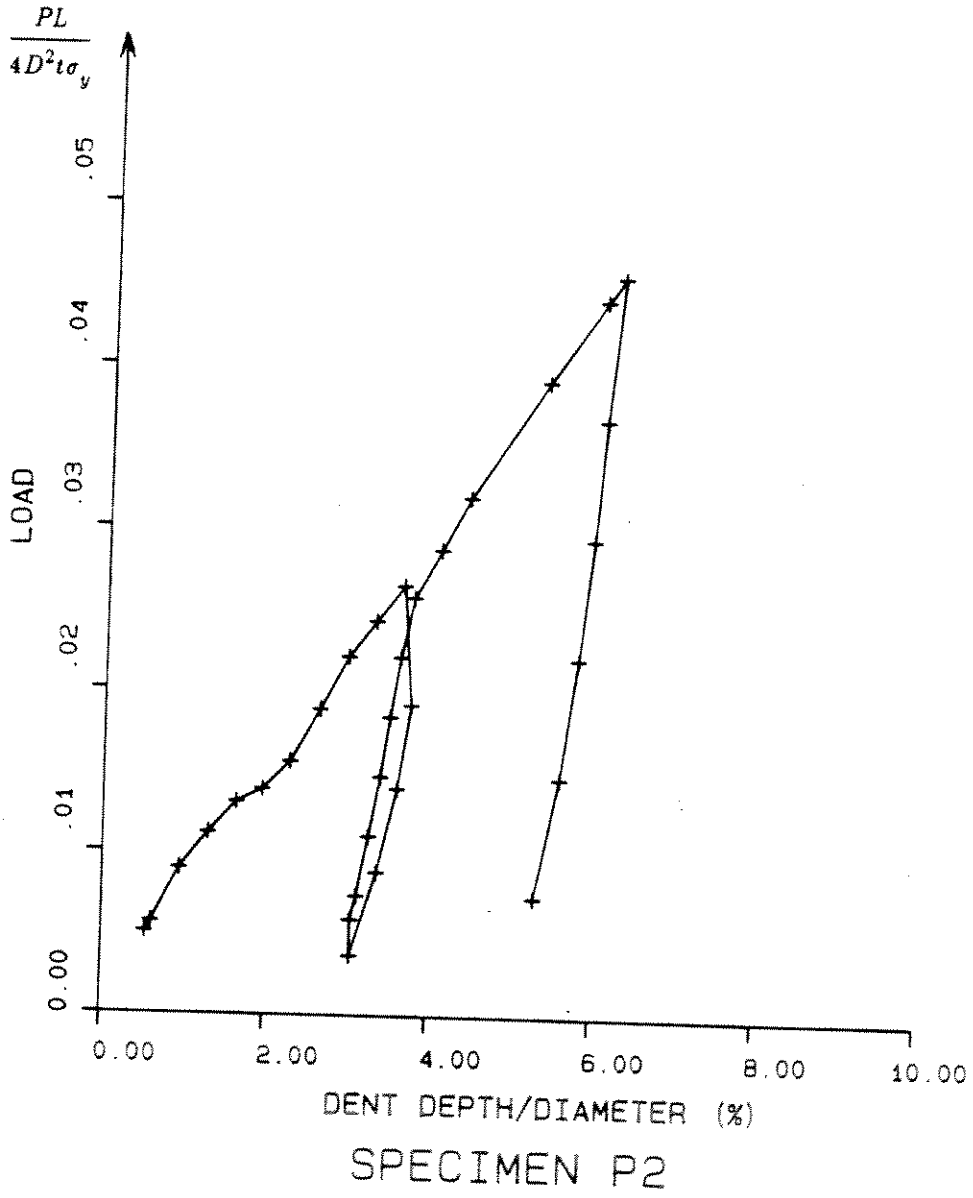

Figure 6: Experimental Load vs. Dent Depth Curve for Specimen P2

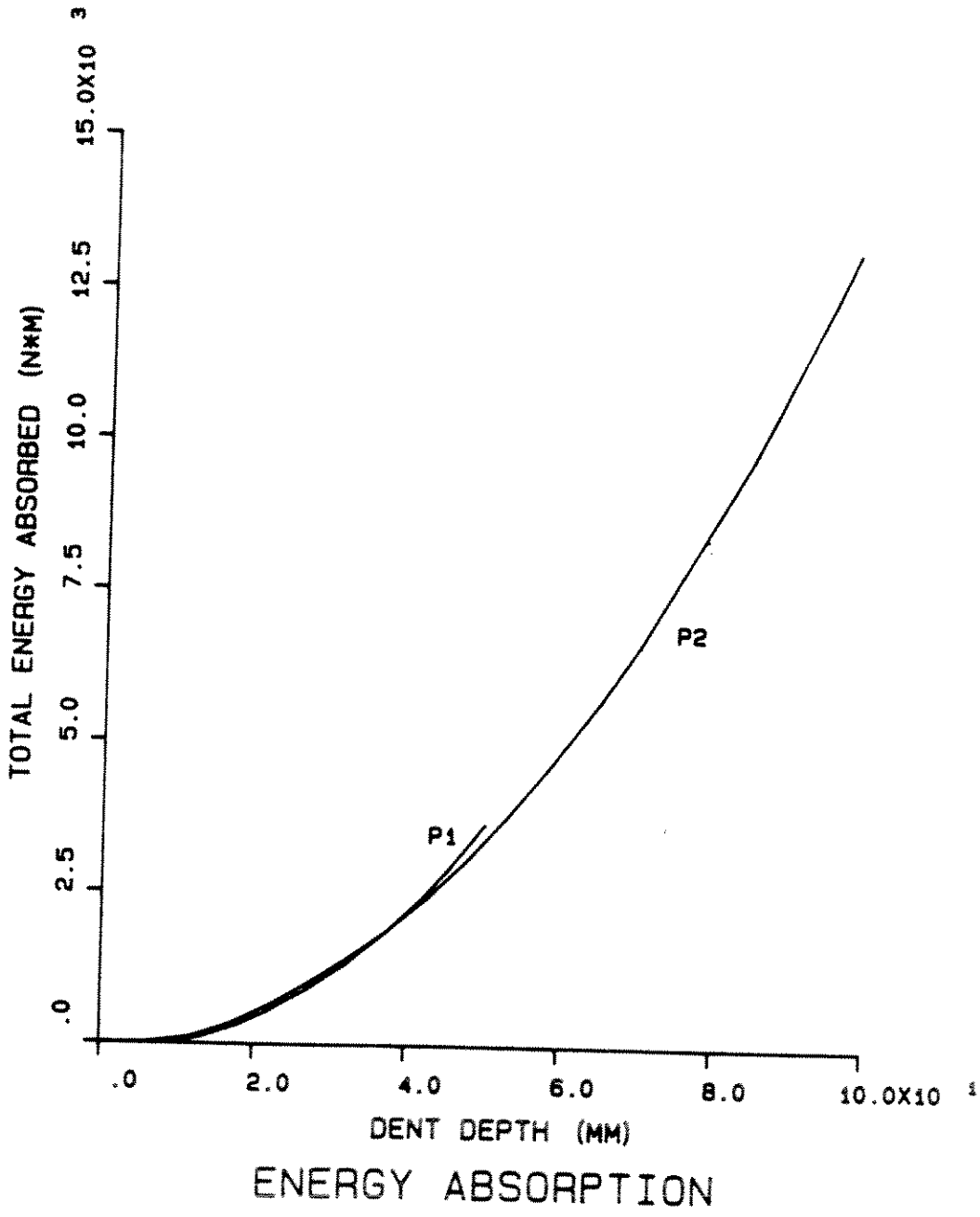

Figure 7: Energy Absorption vs. Dent Depth for Specimens P1 and P2

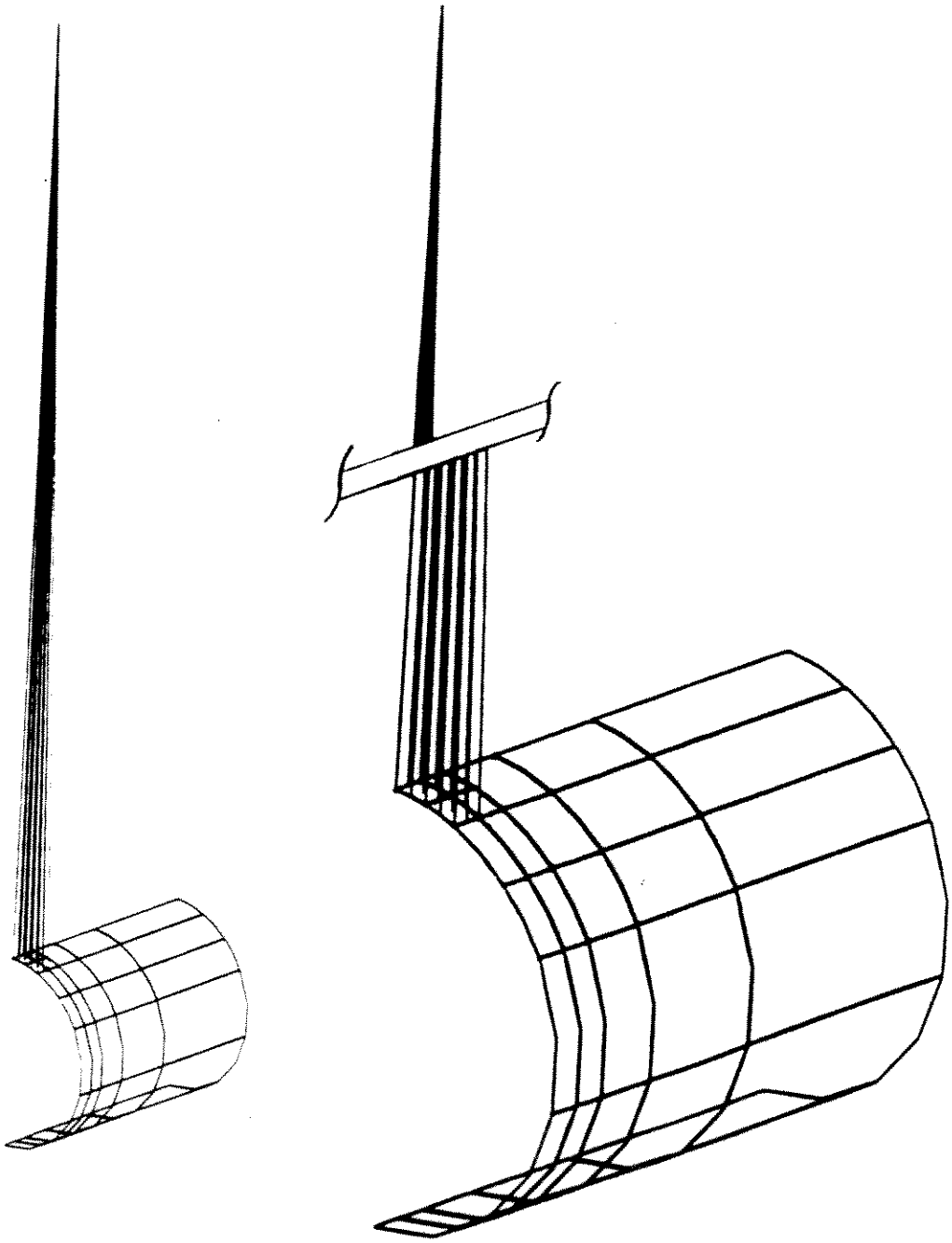

Figure 8: Finite Element Model for Tube Indentation

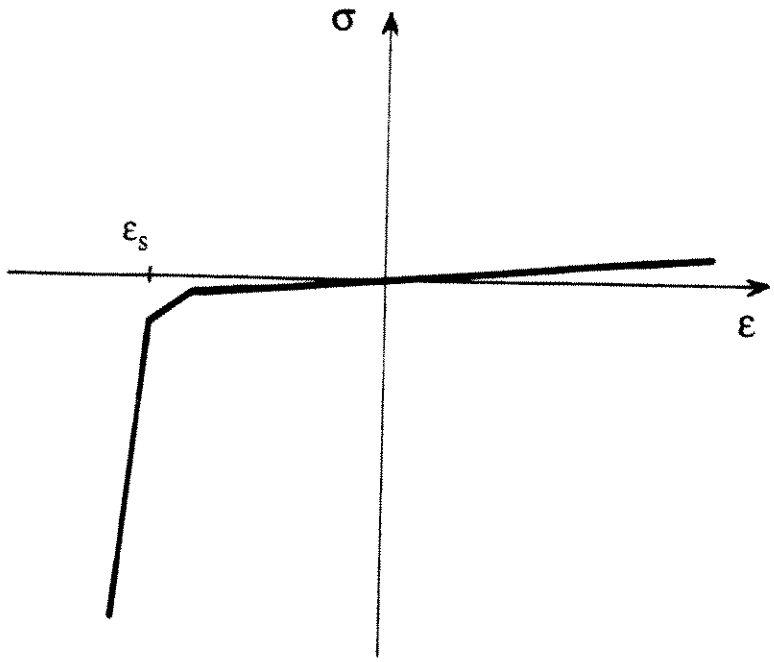

Figure 9: Typical Stress-Strain Relationship for Stiffening Truss Element

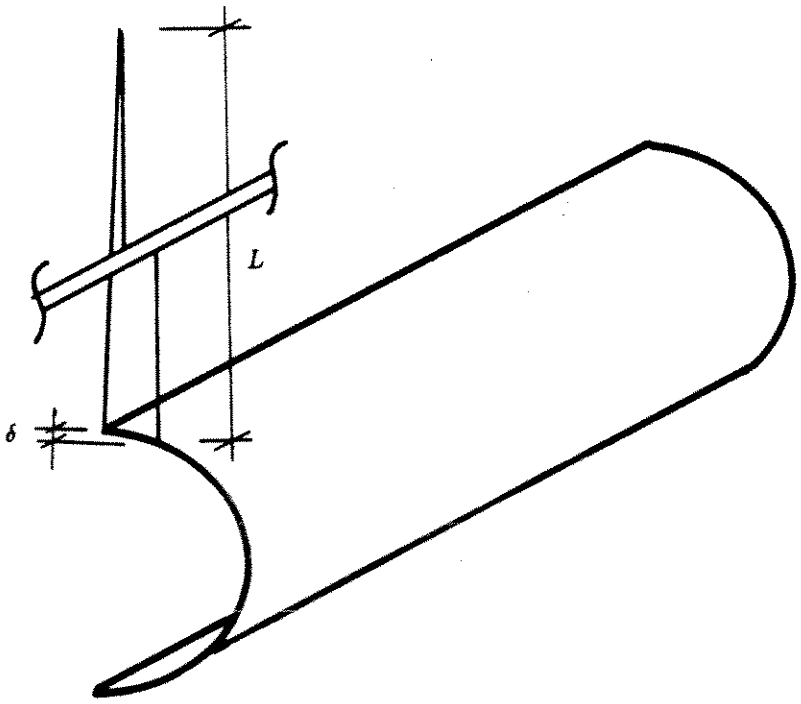

Figure 10: Geometry to Determine ϵ_s

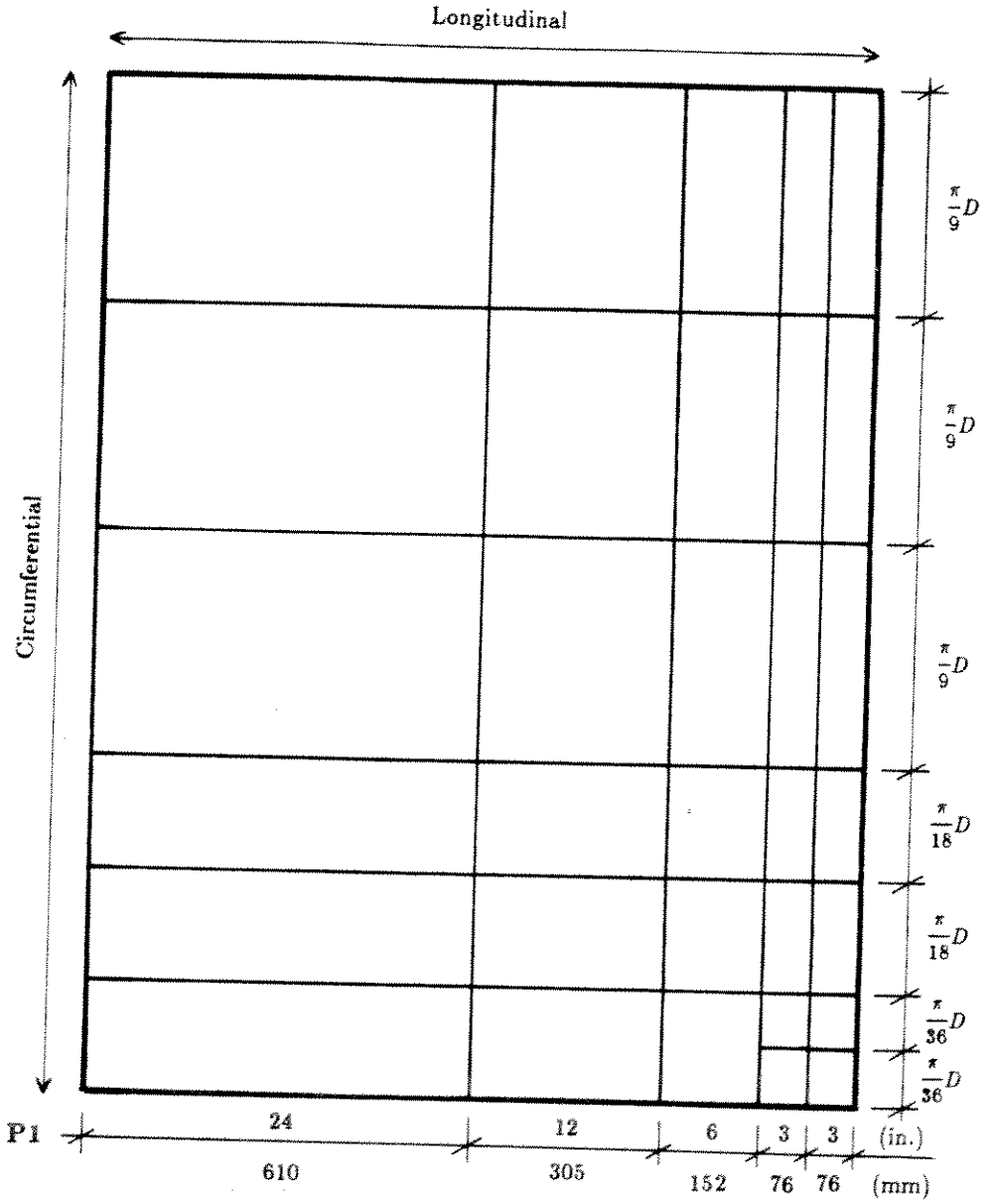

Figure 11: Dimensions for Discretization of Model 2

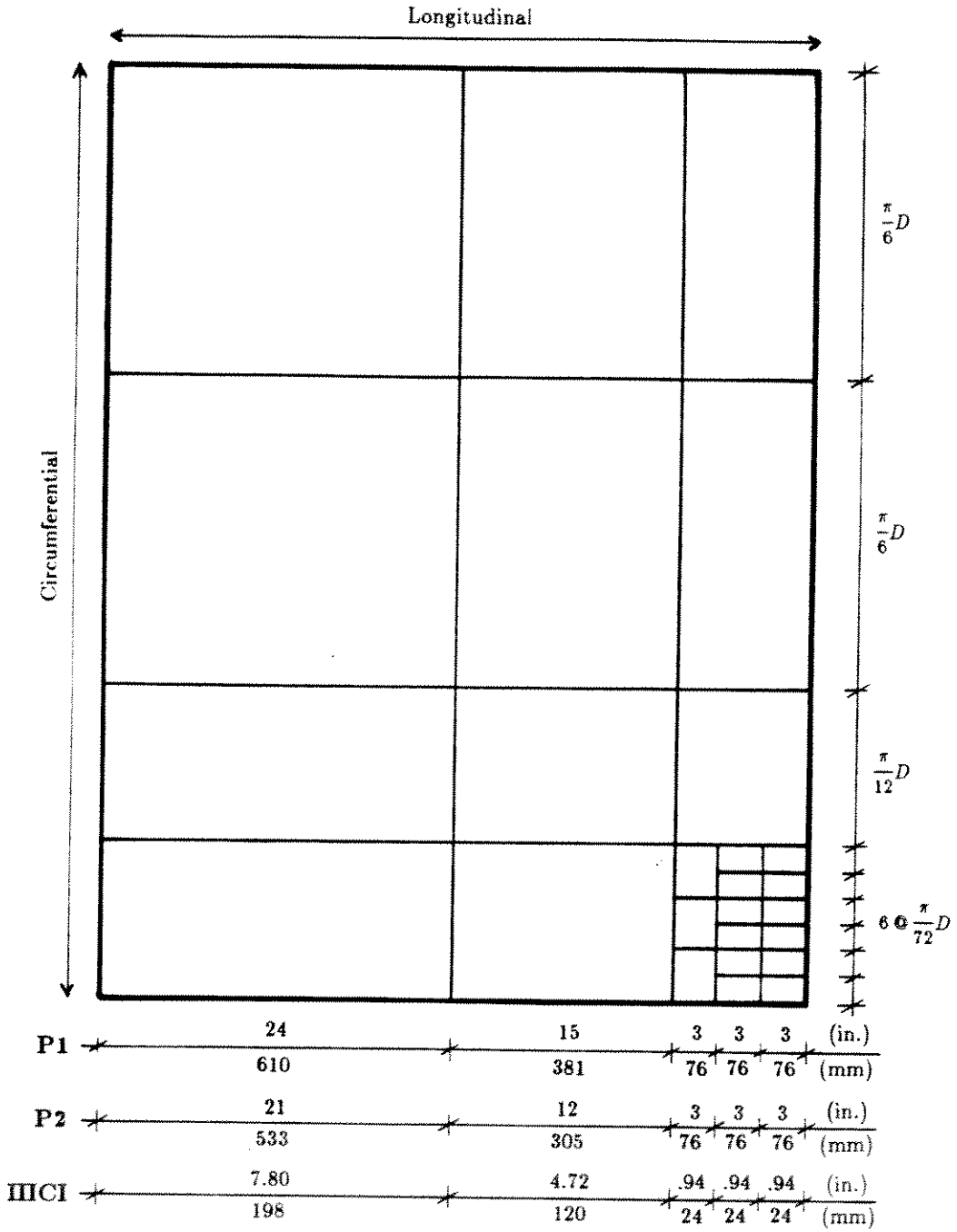

Figure 12: Dimensions for Discretization of Model 4

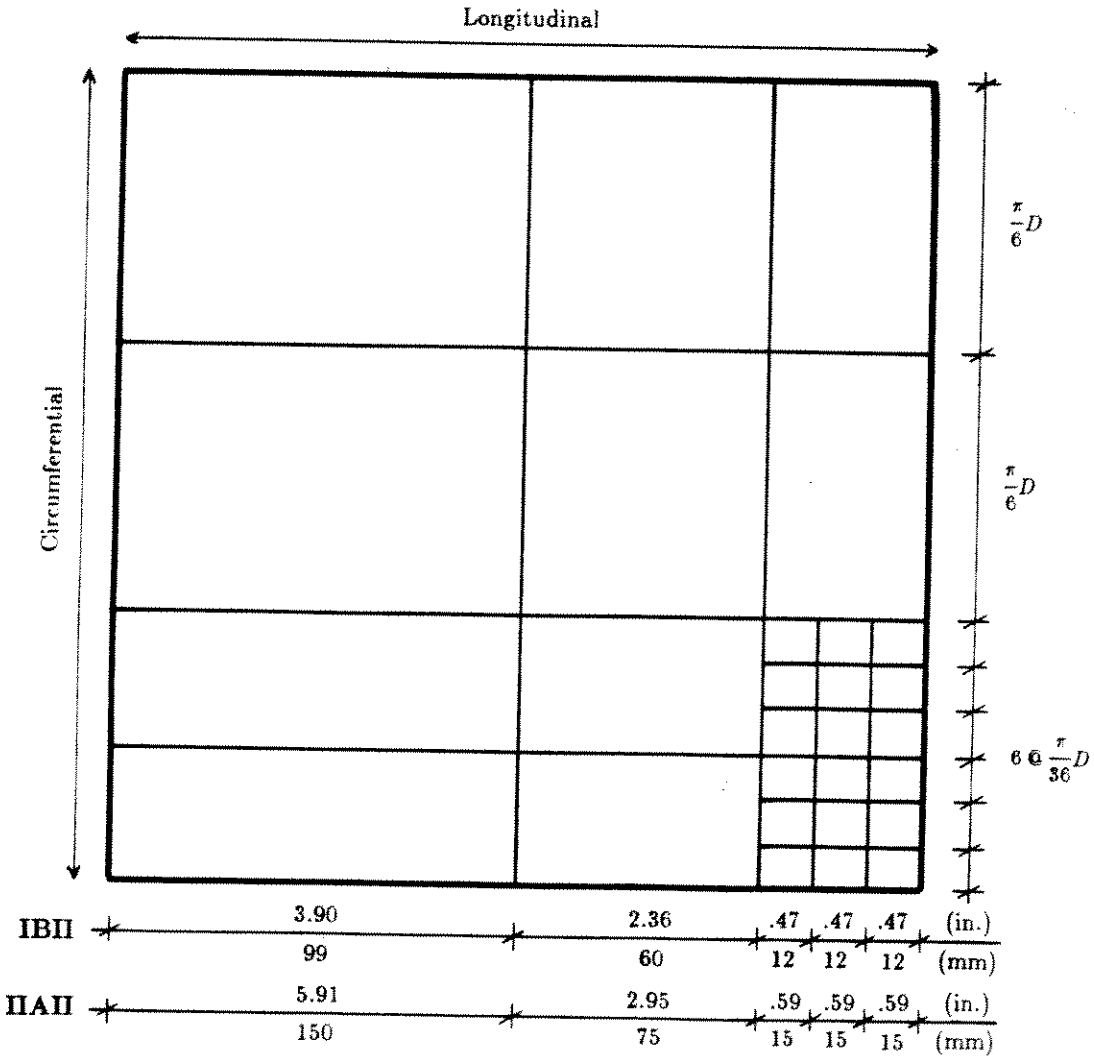

Figure 13: Dimensions for Discretization of Model 8

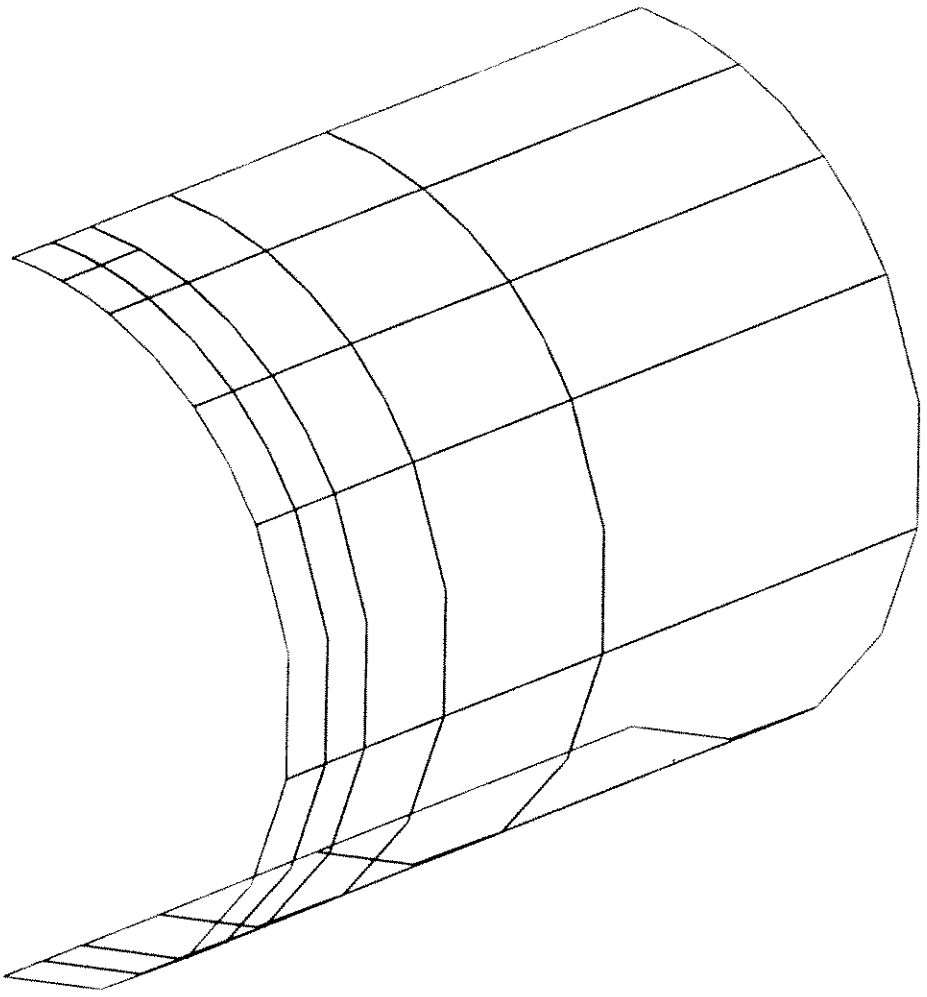

Figure 14: Discretization of Tube - Model 2

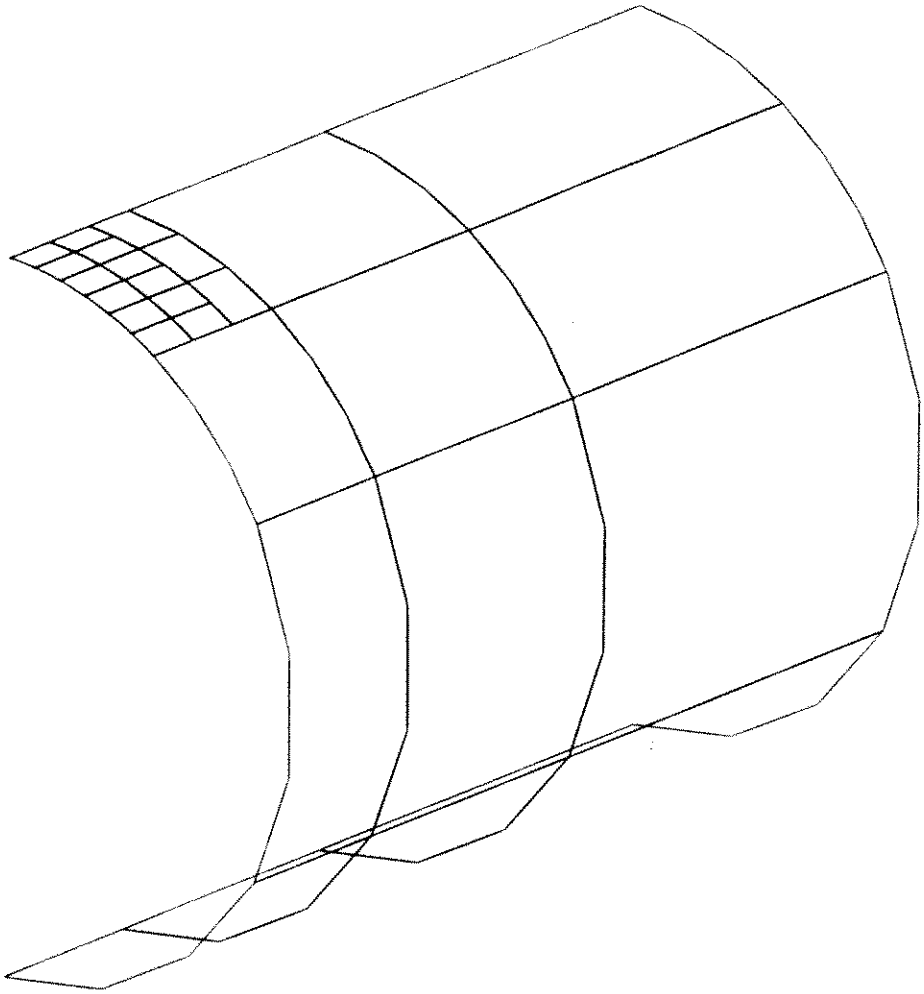

Figure 15: Discretization of Tube - Model 4

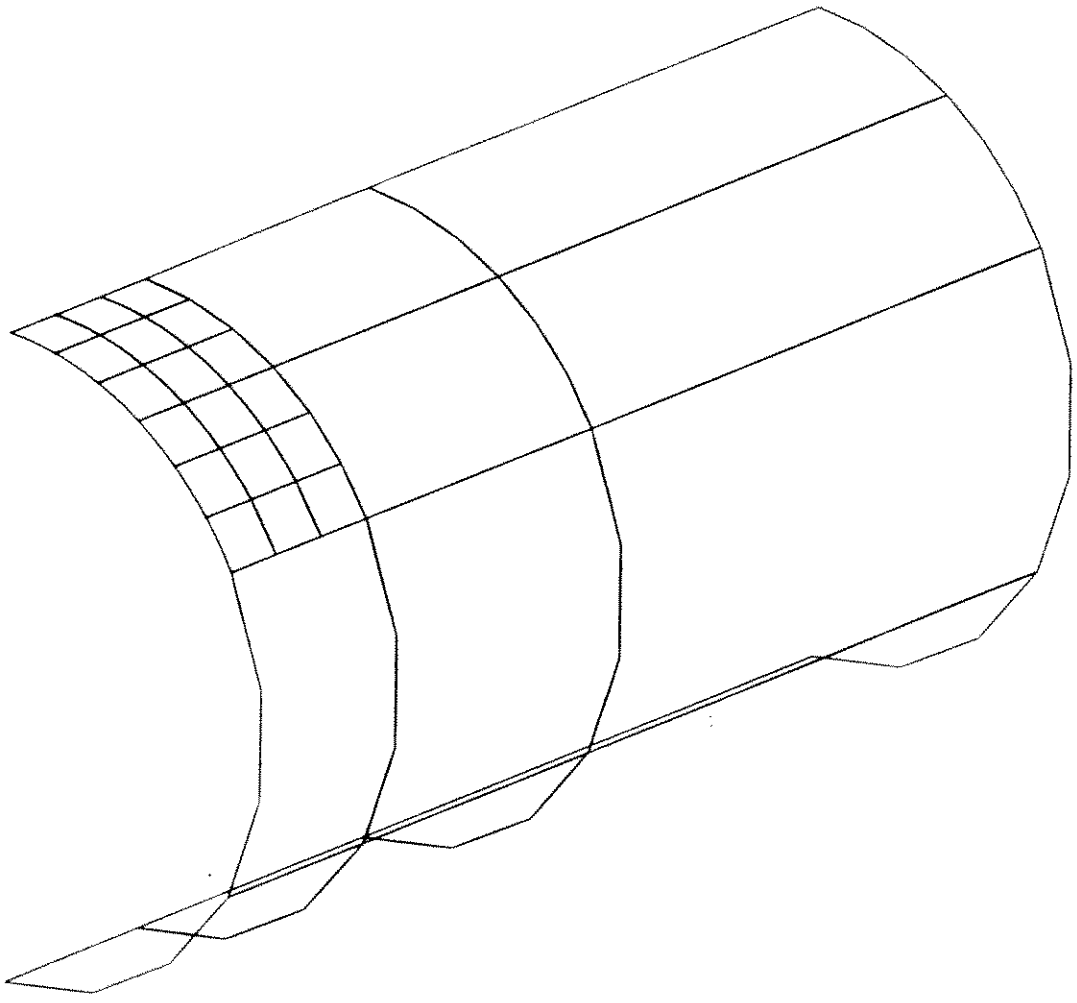

Figure 16: Discretization of Tube - Model 8

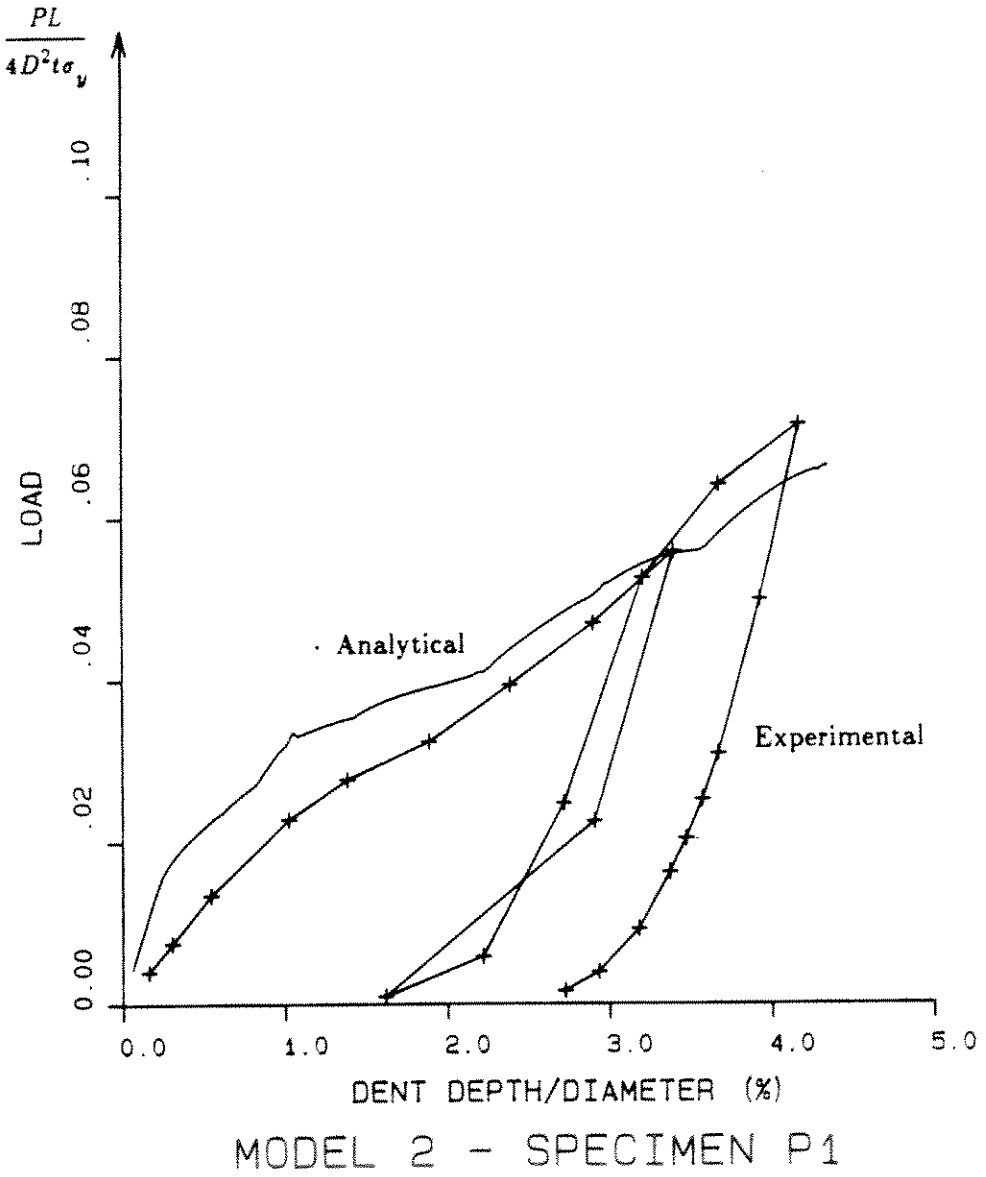

Figure 17: Load vs. Dent Depth, Specimen P1 - Model 2

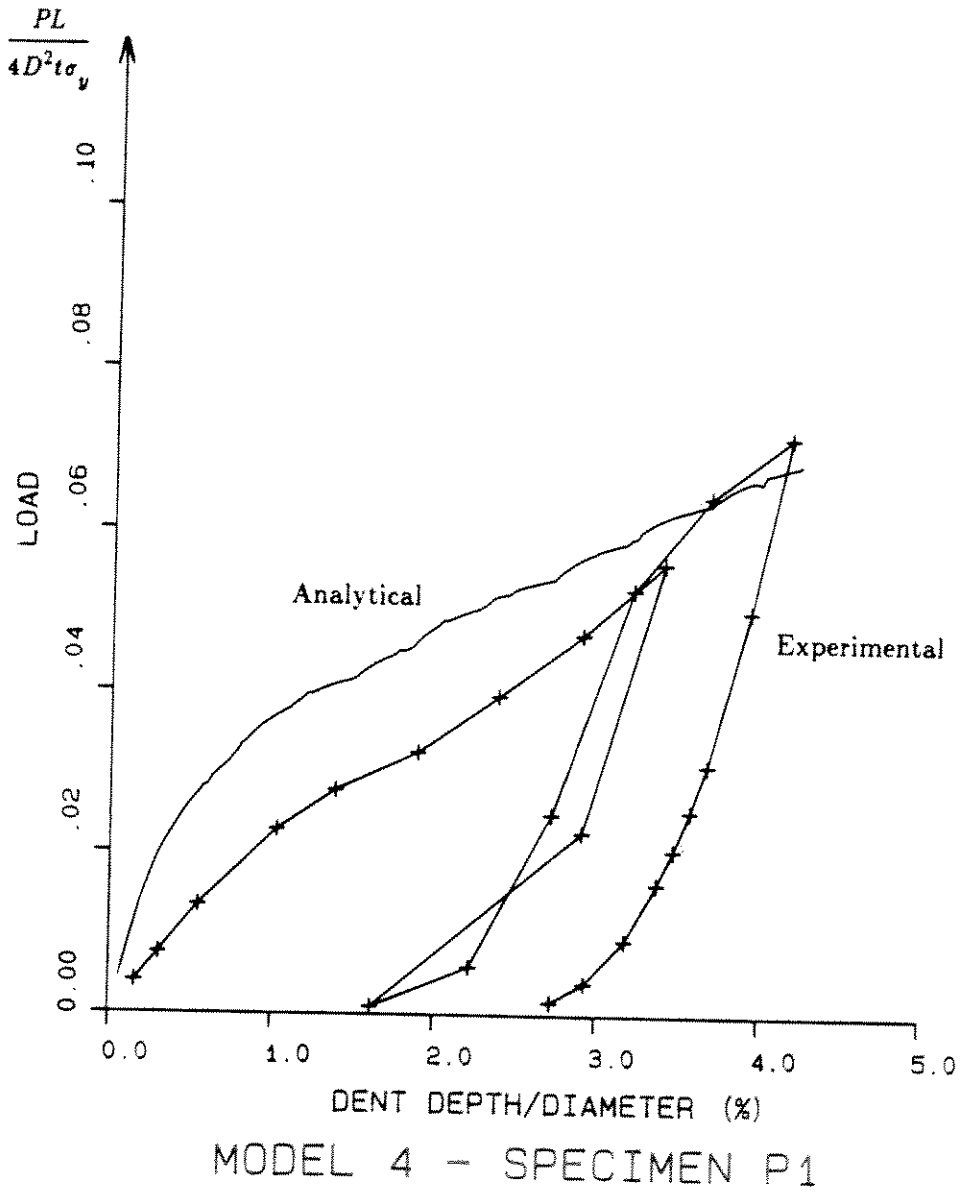

Figure 18: Load vs. Dent Depth, Specimen P1 - Model 4

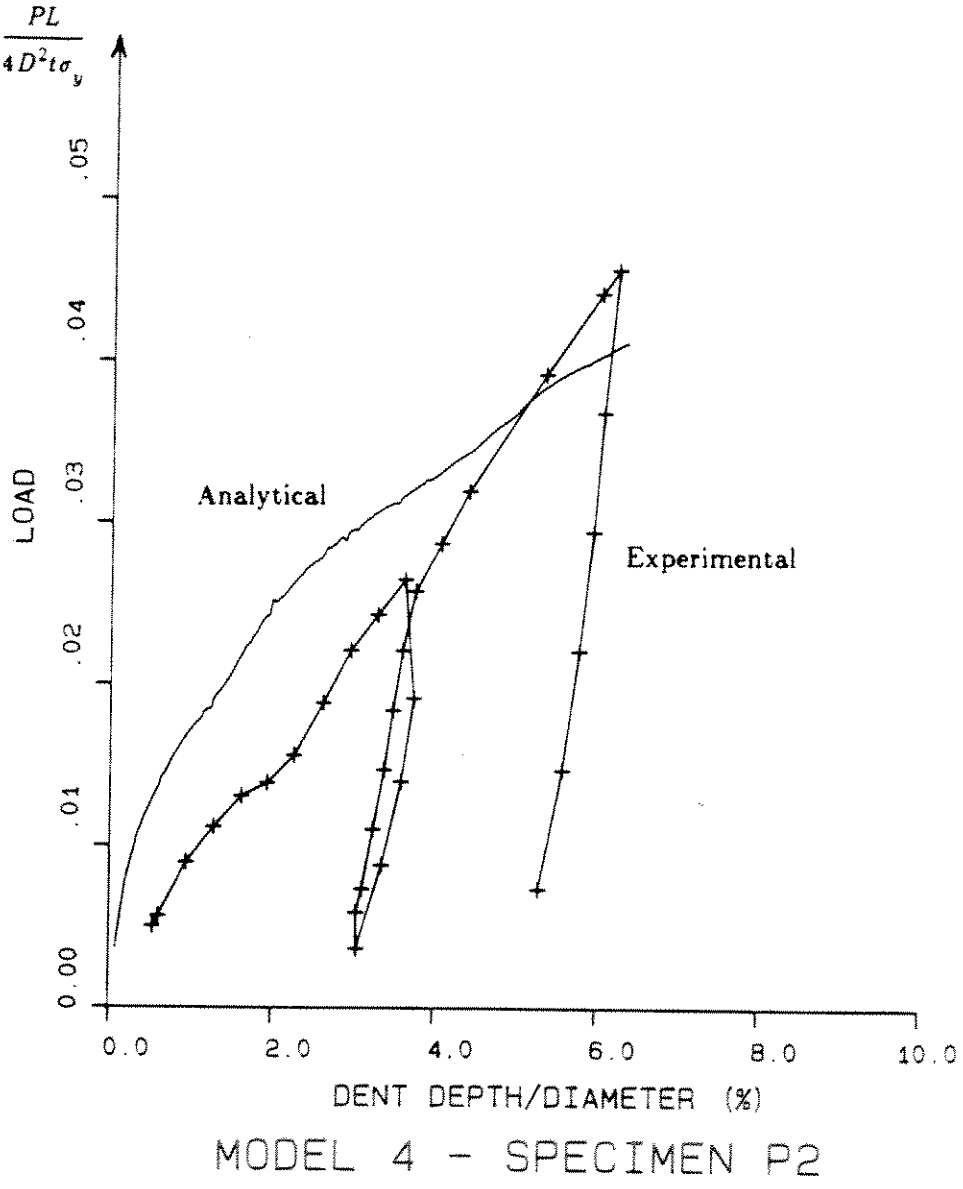

Figure 19: Load vs. Dent Depth. Speicmen P2 - Model 4

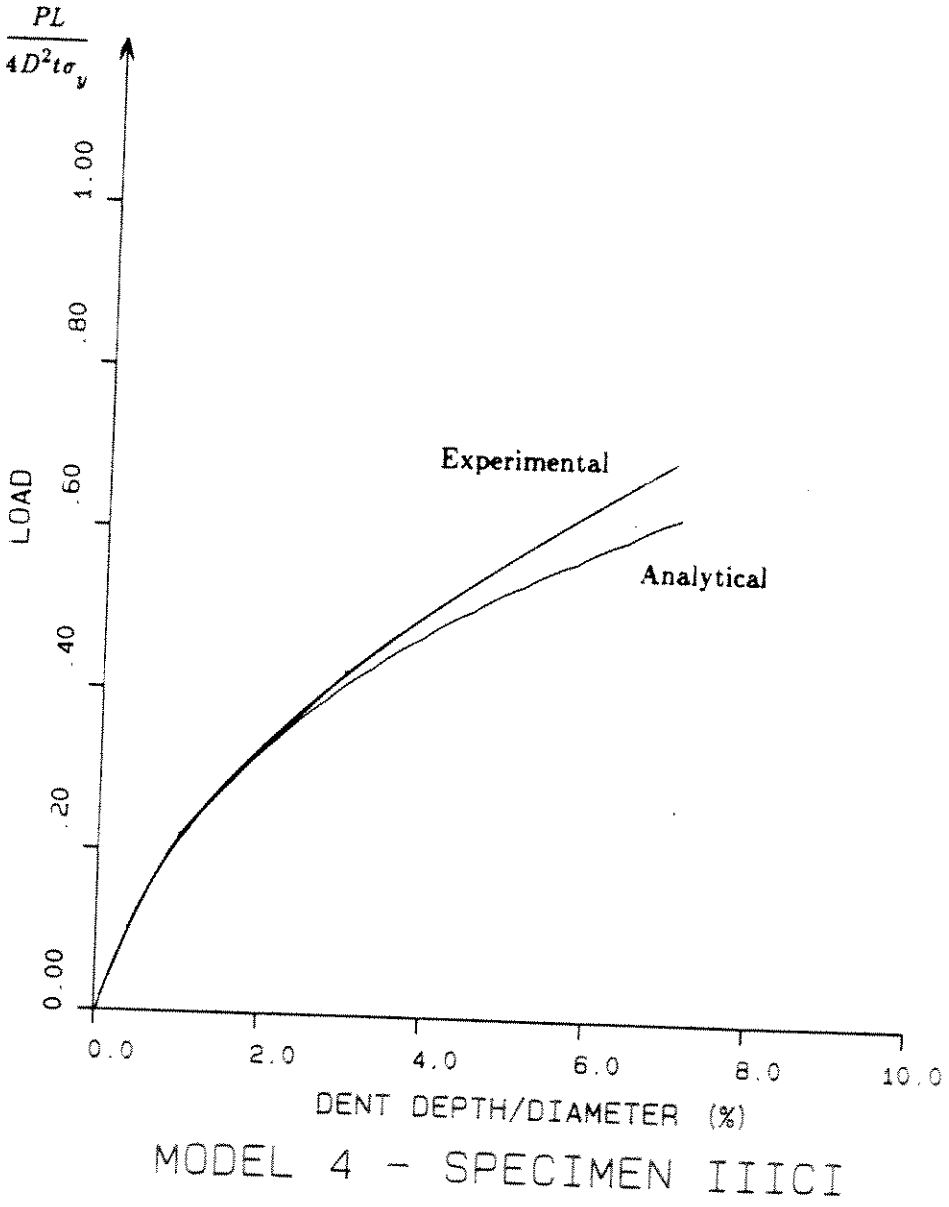

Figure 20: Load vs. Dent Depth, Specimen IIICI - Model 4

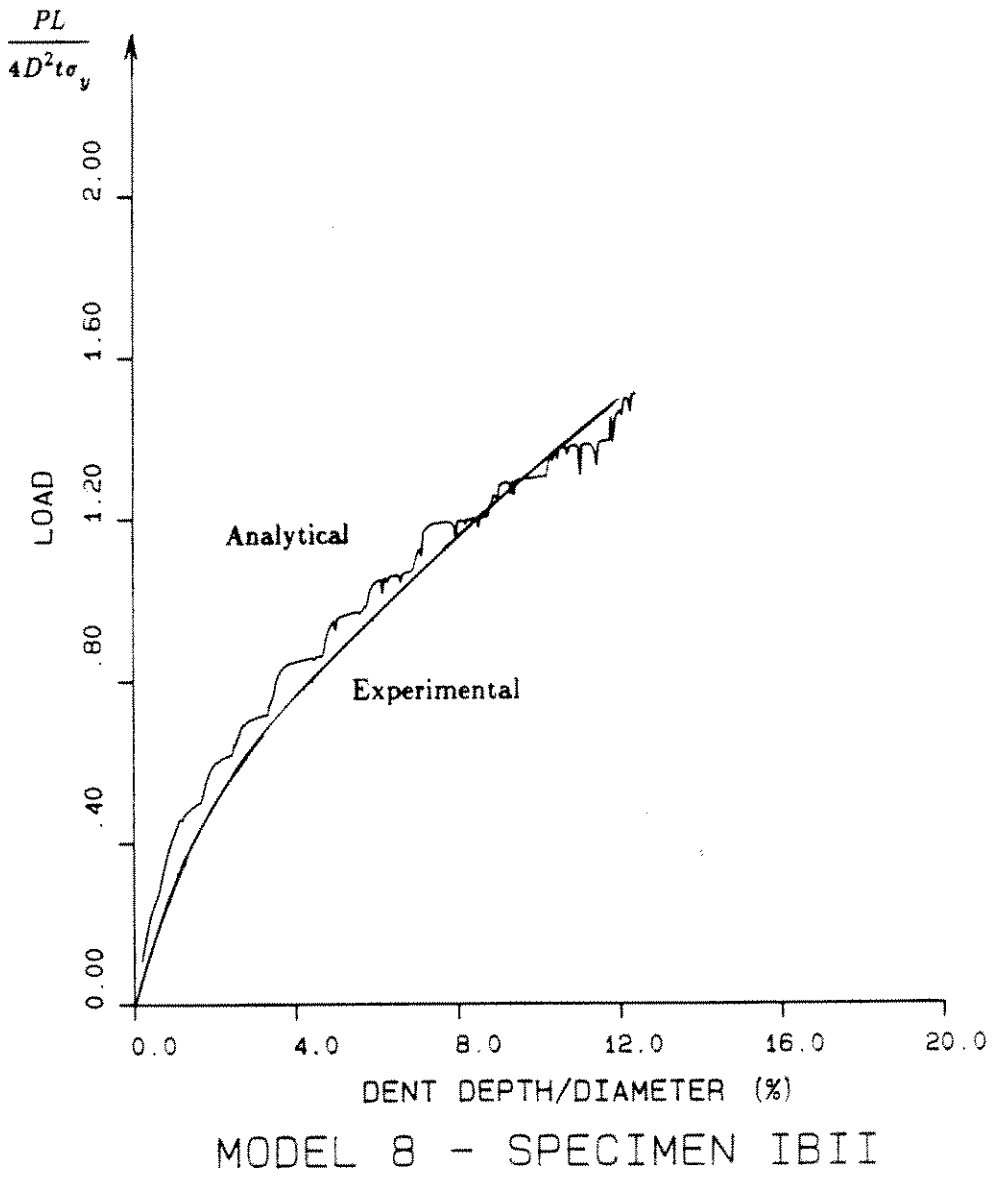

Figure 21: Load vs. Dent Depth, Specimen IBII - Model 8

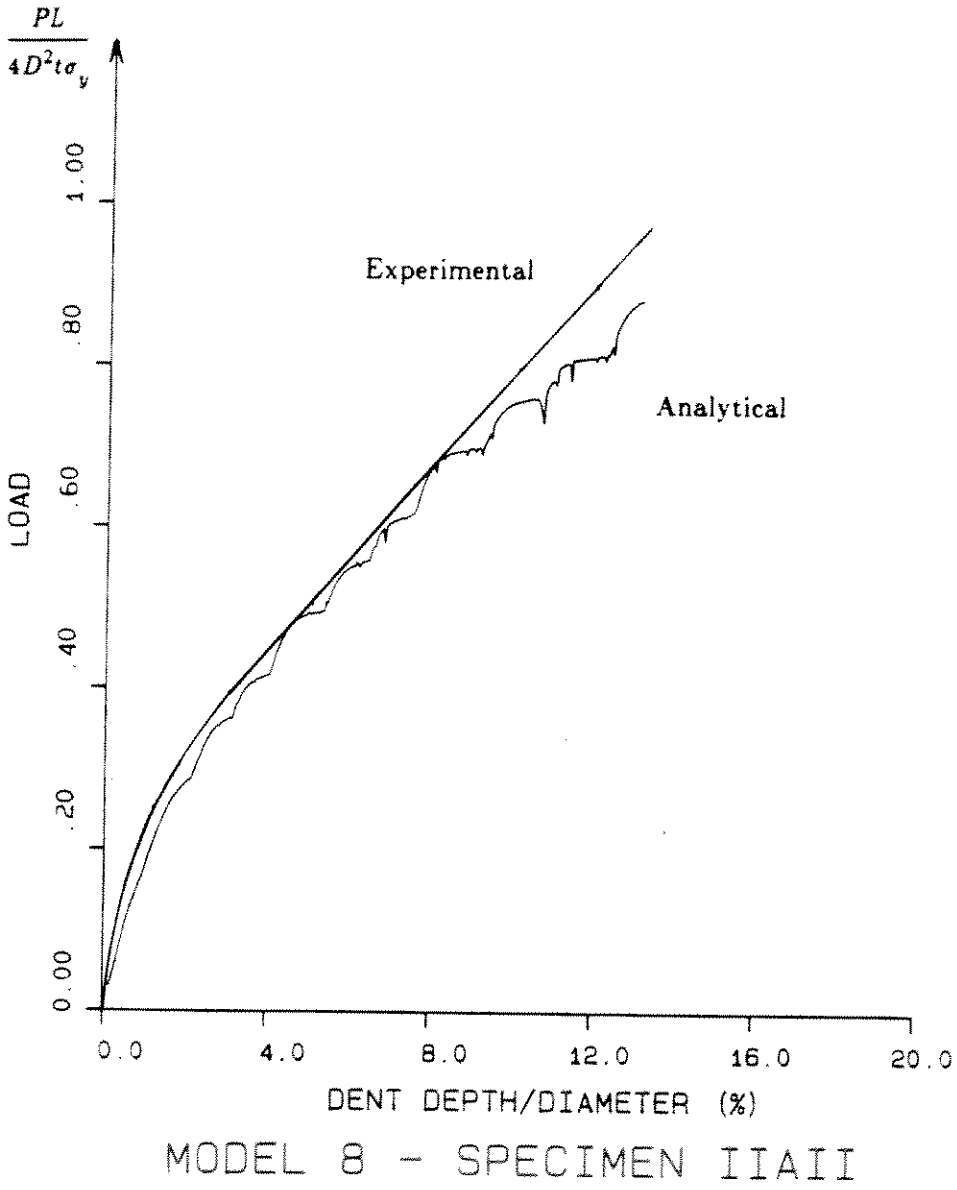

Figure 22: Load vs. Dent Depth. Speicmen IIAII - Model 8

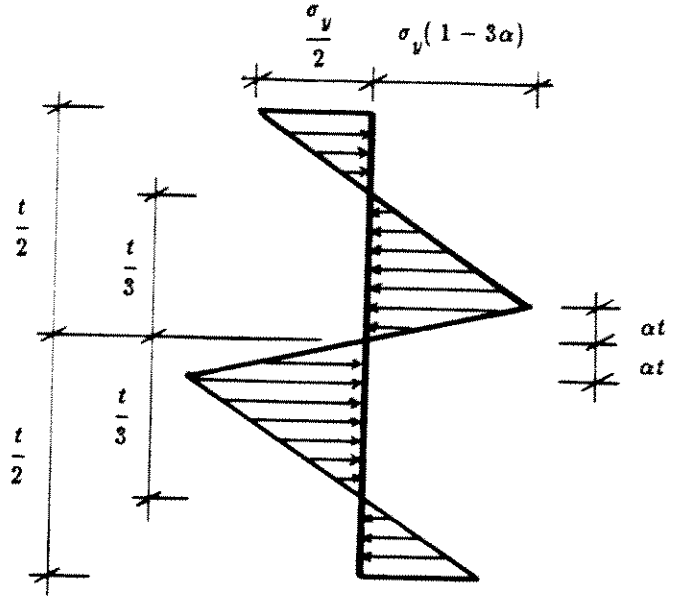

Figure 23: Residual Stresses Through Thickness Due to Cold-Rolling

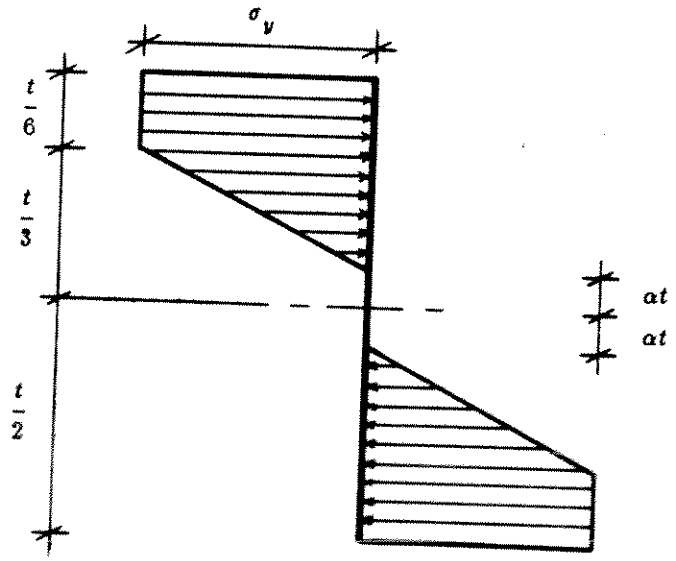

Figure 24: Stress Distribution after Flattening

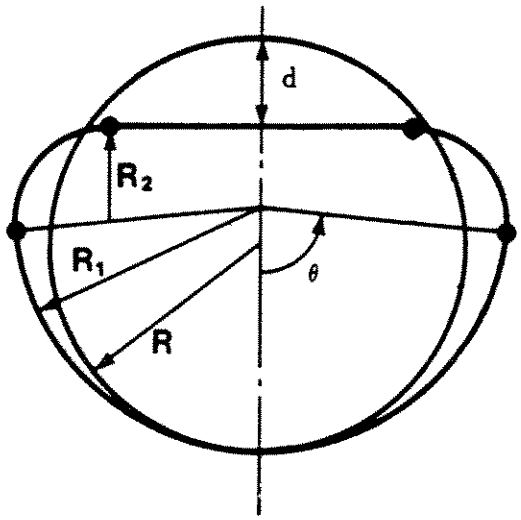

Figure 25: Assumed Deformation of a Ring
(From Reference [17])

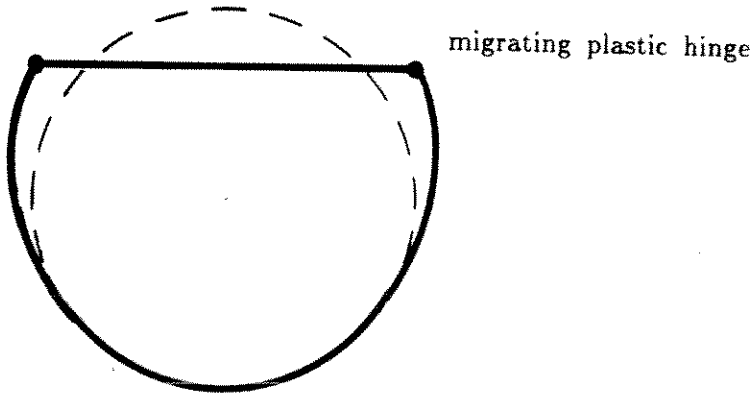

Figure 26: Deformation of a Ring from Idealized Dent Geometry

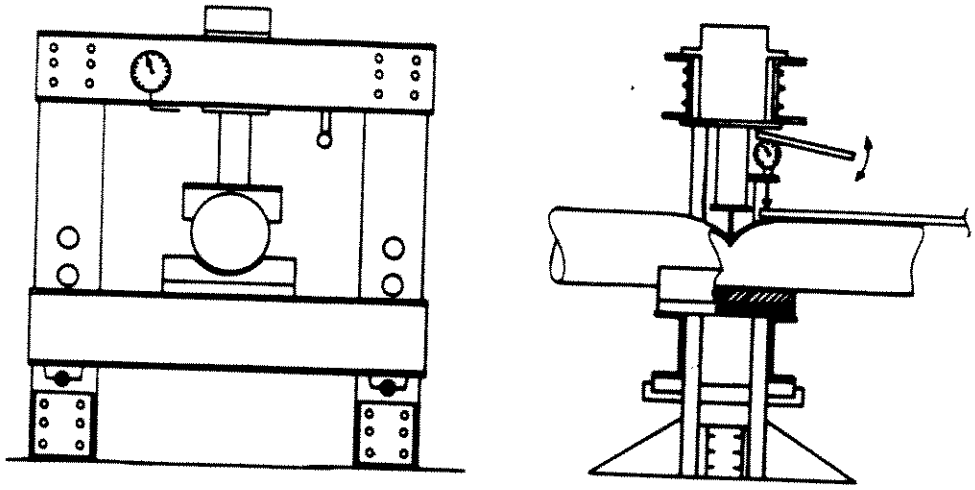

Figure 27: Test Setup for Indentation
(From Reference [14])

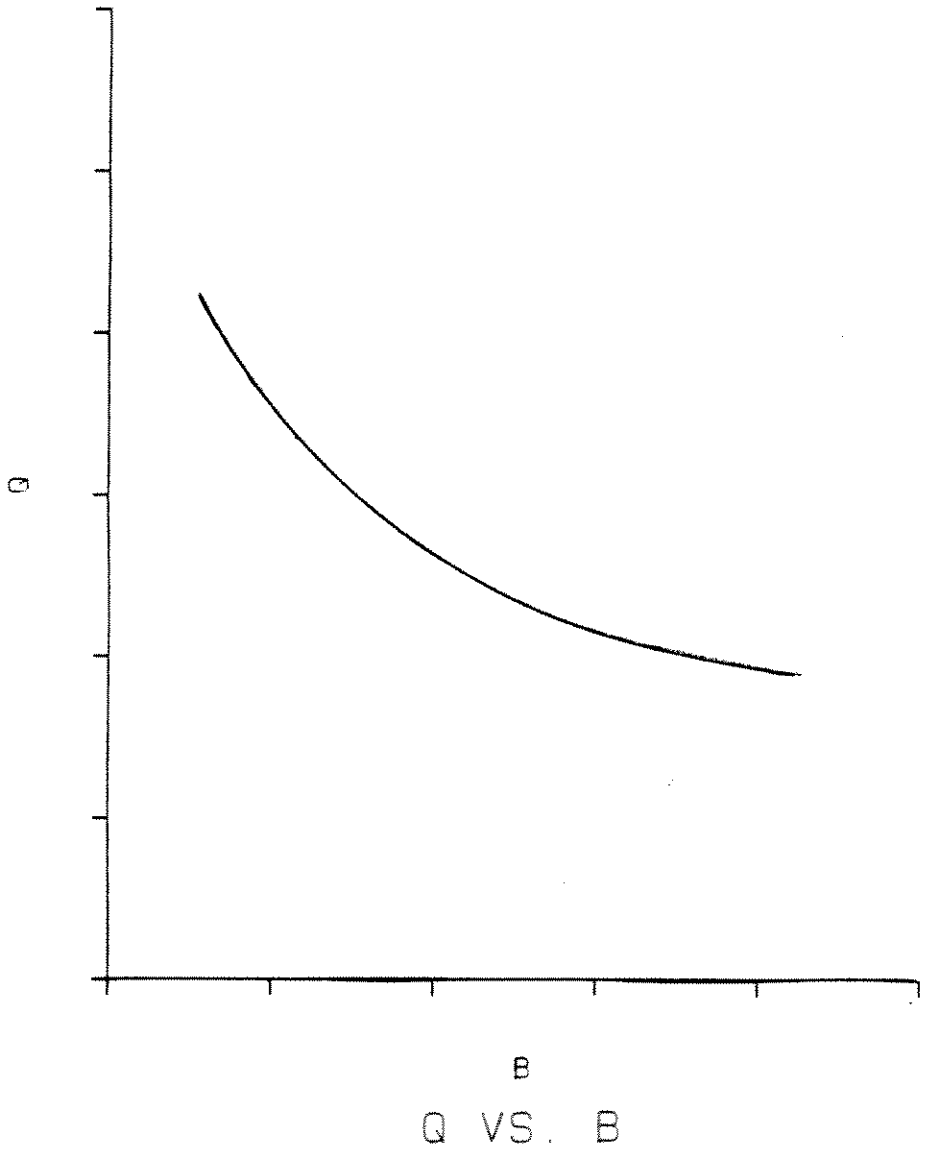

Figure 28: A Typical Q vs. B Relationship

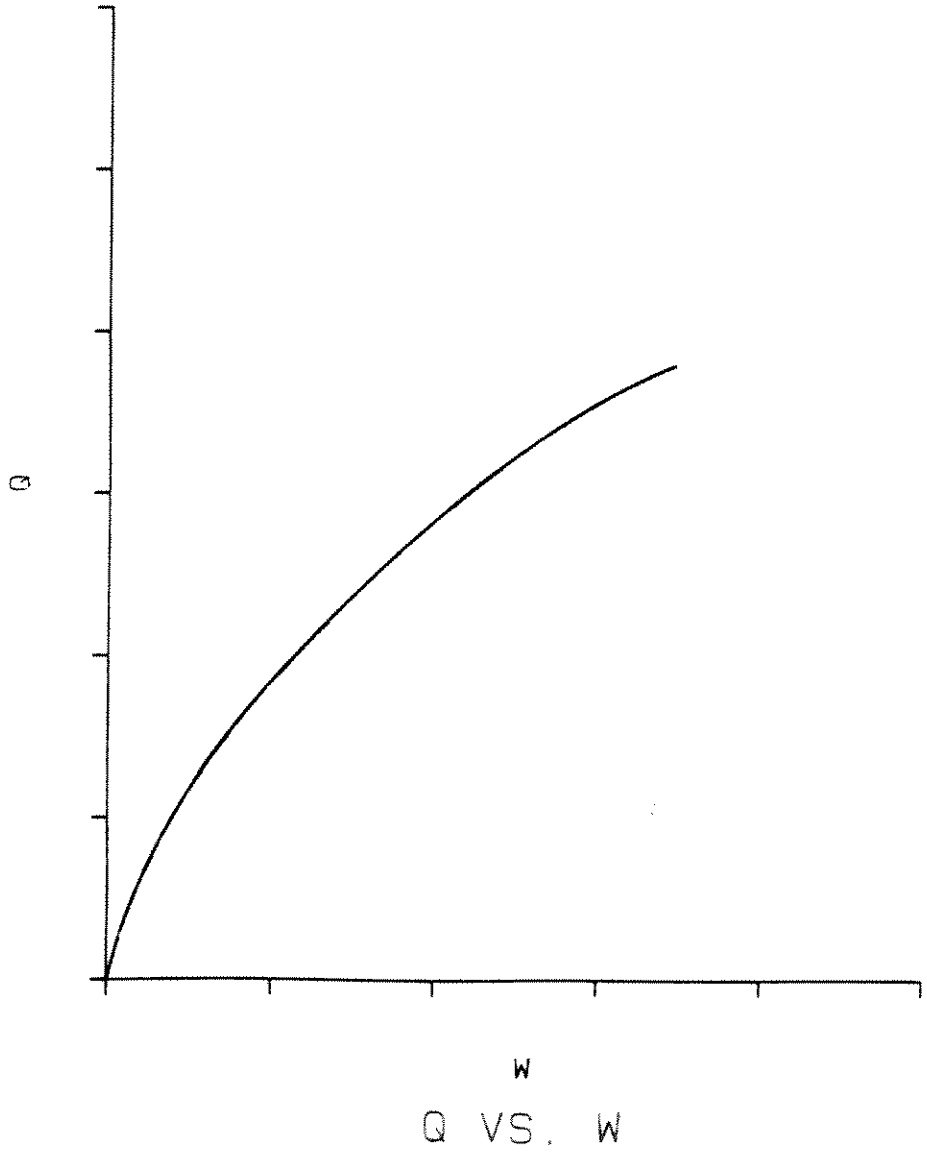

Figure 29: A Typical Q vs. W Relationship

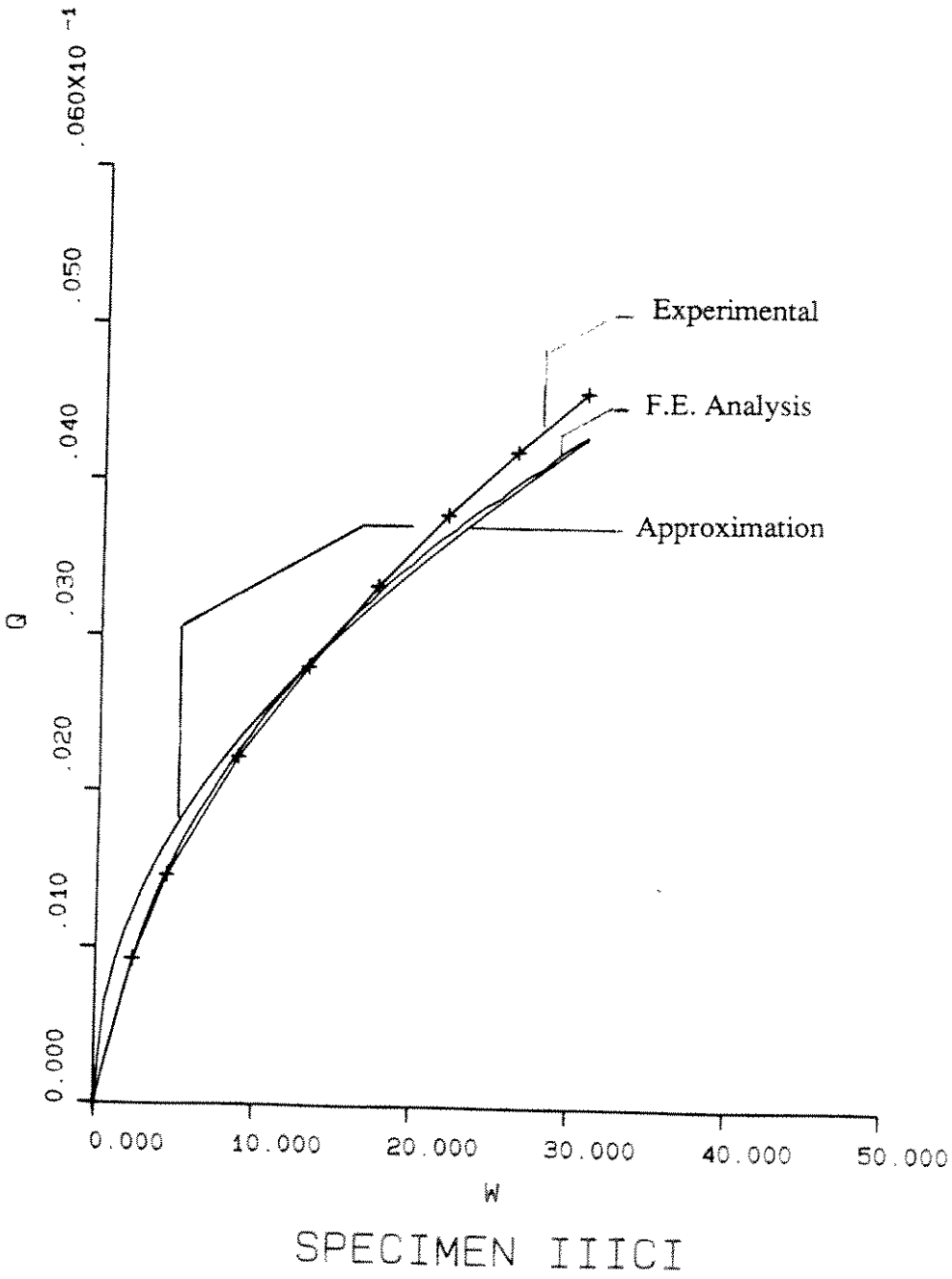

Figure 30: Experimental, Approximate, and Finite Element Q vs. W Relationships for Specimen IIICI

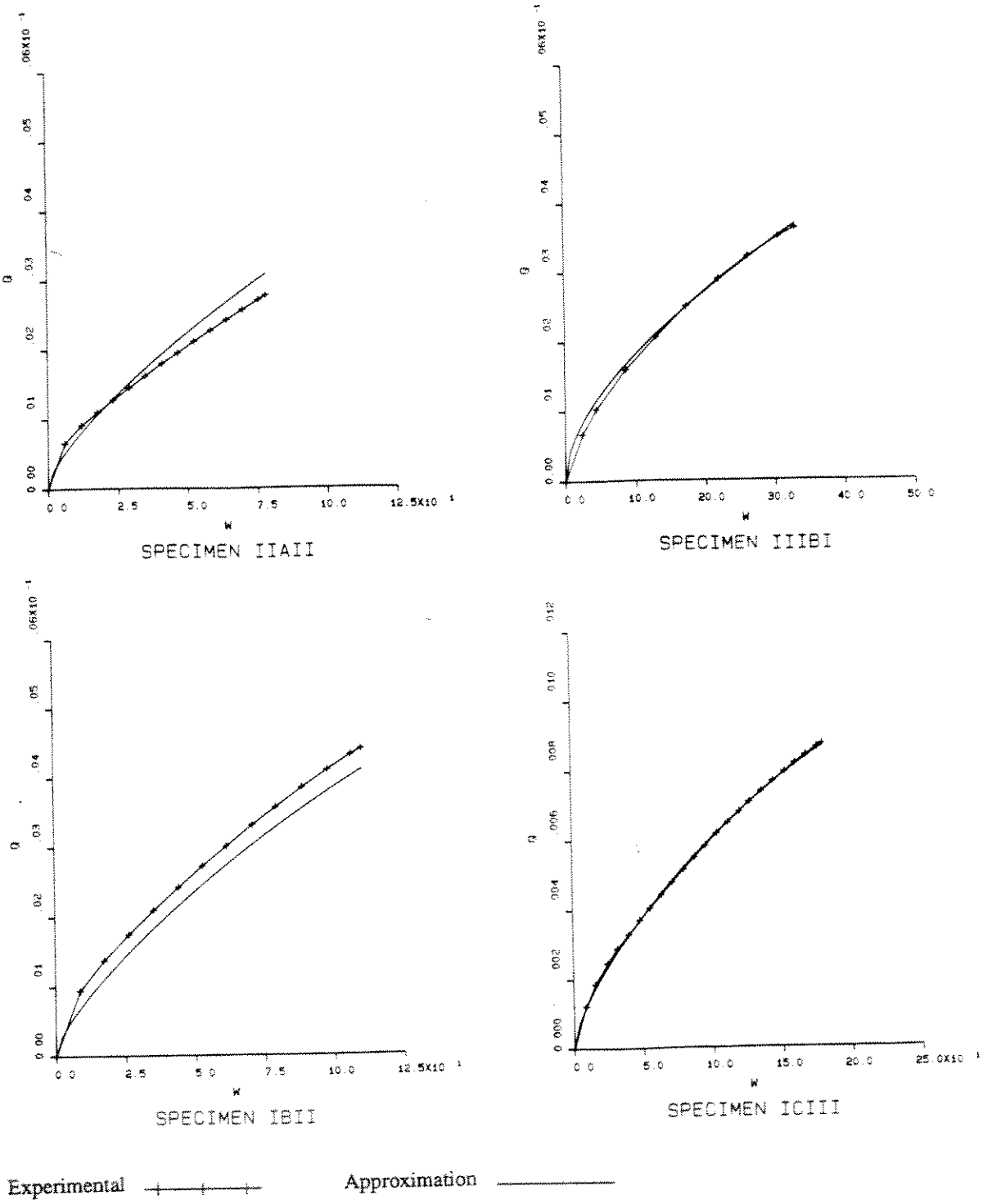

Figure 31: Experimental and Approximate Q vs. W Relationships

References

[1] *ADINA User's Manual*
Report AE 81-1 edition, ADINA Engineering, Inc., 71 Elton Ave., Watertown, Mass. 02172, 1981.

[2] *ADINA System Theory and Modeling Guide*
Report AE 83-4 edition, ADINA Engineering, Inc., 71 Elton Ave., Watertown, Mass. 02172, 1983.

[3] Bathe, K.J.
Finite Element Procedures in Engineering Analysis.
Prentice-Hall, Inc., 1982.

[4] Cook, R.D.
Concepts and Applications of Finite Element Analysis.
John Wiley & Sons, New York, 1981.

[5] Ellinas, C.P., and Valsgard, S.
Collision and Damage of Offshore Structures: A State-of-the-Art.
In *Proceedings of the Fourth International Offshore Mechanics and Arctic Engineering Symposium, Vol. 2*, pages 475-495. American Society of Mechanical Engineers, New York, February, 1985.
(Symposium held in Dallas, TX, on February 17-21, 1985).

[6] Grimm, D.F., and Ostapenko, A.
Local Buckling of Steel Tubular Columns.
In *Proceedings*, pages 25-28. Structural Stability Research Council, Bethlehem, PA, 1982.

[7] Hypponen, P. and Raiko, H.
Experiences in Nonlinear Shell Analysis Using Adina.
Computers and Structures 17(5-6):649-652, 1983.

[8] Ostapenko, A., and Grimm, D.F.
Local Buckling of Cylindrical Tubular Columns Made of A-36 Steel.
Fritz Engineering Laboratory Report No. 450.7, Lehigh University, Bethlehem, PA, February, 1980.

[9] Ostapenko, A., and Surahman, A.
Structural Element Models for Hull Strength Analysis.
Fritz Engineering Laboratory Report No. 480.6, Lehigh University, September, 1982.

[10] Padula, J.A., Ostapenko, A.
Indentation Behavior and Axial Tests of Two Tubular Columns.
Fritz Engineering Laboratory Report No. 508.5, Lehigh University, Bethlehem, Pennsylvania, 1987.

[11] Padula, J.A. and Ostapenko, A.
Indentation Behavior and Axial Tests of Two Tubular Columns.
In *Proceedings of Offshore Technology Conference-1987*, pages 151-159. Offshore Technology Conference, April, 1987.
OTC 5438.

[12] Sherman, D.R.
Tests of Circular Steel Tubes in Bending.
Journal of the Structural Division, ASCE 102(ST11, Paper 12568):2181-2195, November, 1976.

[13] Soares, C.G., and Soreide, T.H.
Plastic Analysis of Laterally Loaded Circular Tubes.
Journal of Structural Engineering, ASCE 109(2):451-467, February, 1983.

[14] Taby, J., and Rashed, S.M.H.
Experimental Investigation of the Behaviour of Damaged Tubular Members.
Technical Report MK/R92, Department of Naval Architecture and Marine Engineering, The Norwegian Institute of Technology, Trondheim, Norway, 1980.

[15] Taby, J., and Moan, T.
Collapse and Residual Strength of Damaged Tubular Members.
Behaviour of Offshore Structures.
Elsevier Science Publishers B.V., Amsterdam, 1985, pages 395-408.

[16] Thomas, S.G., Reid, S.R., and Johnson, W.
Large Deformations of Thin-Walled Circular Tubes under Transverse Loading-I.
International Journal of Mechanical Sciences 18(6):325-333, June, 1976.

[17] Wierzbicki, T., and Suh, M.S.
Denting Analysis of Tubes Under Combined Loading.
Technical Report MITSG 86-5, MIT Sea Grant College Program, Massachusetts Institute of Technology, 77 Massachusetts Ave., Cambridge, MA 02139, March, 1986.
NA84AA-D-0046 R/O-19.

Appendix A
Experimental Work by Others

Experimental data reported by other researchers was used to assess the validity of the finite element analysis and to use as a database in developing a simplified analytical procedure. Specifically, the indentation behavior of three specimens selected from Reference [14] (Specimens IIICI, IBII, and IIAII) was analyzed. The experimental work on these three specimens is described here since the details are relevant to understanding the conclusions drawn from the analytical work.

A.1 Scope

The principal source of experimental data was Reference [14]. This work covered indentation and axial load tests of 24 tubular members and included the experimental load vs. dent depth curves as well as a comparison of the theoretical and experimental axial strengths of the dented specimens.

A.2 Description of Test Specimens

The test specimens were cold-drawn manufactured seamless tubes which were heat treated to relieve residual stresses from the manufacturing process and improve ductility.** The heat treatment consisted of heating to 550 °C (1020 °F) for one hour followed by slow cooling.

The specimen geometries were representative of a 1:4 scaling of members commonly found in offshore structures. The D/t ratios of the specimens varied from 40 to 64 with diameters ranging from 125 to 250 mm (5 to 10 in.). All specimens had the same length of 3500 mm (138 in.). The dent depth of the specimens ranged from 2% to 20% of the diameter.

**Pertinent information, including geometric data and material properties of the three specimens analyzed in the current program, is listed in Table 1.

A.3 Indentation of Specimens

The method of indentation of the specimens was different from that used for Specimens P1 and P2 of the current study. The objective was to produce specimens without overall bending deformations so that the effect of indentations could be isolated. To accomplish this, the tubes were supported in a wooden cradle directly below the indenter as shown in Fig. 27. The denting force was transmitted to the tube through a "knife edge" (5 mm radius) indenter. During indentation, the dent depth and the load, provided by a hydraulic jack, were measured with a dial gage and manometer, respectively. Although not indicated on the load vs. dent depth curves presented in the reference, the specimens required multiple load cycles to produce the desired dent depths.

The type of support and the "knife edge" loading were the principal variations in modeling these specimens for the finite element analysis in comparison with Specimens P1 and P2.

Appendix B

Nomenclature

B	Member geometry parameter $= \left(\frac{D}{t}\right)^2 \frac{E}{\sigma_y}$
D	Diameter
d	Dent Depth
L	Length
P	Lateral Load (Denting Load)
Q	Load parameter $= \frac{P}{D^2 \sigma_y}$
R	Radius
R_1,R_2	Radii as defined in Fig. 26
r_2	Nondimensionalized Radius $= \frac{R_2}{R}$
t	Thickness of Tube Wall
W	Deformation (dent depth) parameter $= \frac{d E}{D \sigma_y}$
α	Coefficient $= \frac{D \epsilon_y}{2t} + 3\epsilon_y$
δ	Gap Distance between indenter and tube wall
ϵ	Strain
ϵ_y	Yield Strain
Φ	Curvature
Φ_y	Yield Curvature $= \frac{2\epsilon_y}{t}$
σ	Stress
σ_y	Yield Stress
θ	Angle as defined in Fig. 26